NTNU

Norwegian University of
Science and Technology

The Value of Snow Measurements in Scheduling of Hydropower Plants

Heidi Liljeblad Ødegård

Master of Science in Physics and Mathematics
Submission date: June 2016
Supervisor: Jo Eidsvik, MATH

Norwegian University of Science and Technology
Department of Mathematical Sciences

Abstract

The main goal of the thesis is to study the value of snow measurements in the scheduling of hydropower plants. This is done by implementing an approximative Least-Square Monte Carlo(LSMC) method to calculate the scheduling. The optimization algorithm uses dynamic programming to find the optimal strategy. The spot price is deterministic, while the inflows are stochastic. Snow measurements are then included in the model, to calculate the Value of Information. Realistic data from a large-size Norwegian power plant is used to fit a normal distribution to simulate different inflow scenarios used in the model. The correlation between the snow measurements and the inflows are also studied to see how different snow levels influence the inflows in the flood period.

The analysis of the data showed that the maximum amount of snow and the total inflow in the flood period, week 16-32, is highest correlated with a correlation coefficient equal 0.85. The numerical testing of the LSMC-method showed that the spot price and the ratio between the total inflow and the upper reservoir limit have the biggest impact on the optimal strategy. The value of the snow measurements vary for different parameters in the model. When the reservoir is big compared to the total inflow, the snow has no value. When the reservoir is smaller, the probability for overflow is bigger and the snow measurements are valuable. The increase in value by using the snow measurements variates between 0 and 10 %. The annual production in Norway is 130 TWh, worth more than 4 billions NOK. This means that even a small improvement results in a big revenue.

If 40 % of the snow measurements are uncertain and in average 10% higher or lower than the real snow reservoir, the value of the measurement decreases with 25 %. The value was also calculated for different correlation coefficients 0.55 and 0.25, and the value of the measurements decreased with 24 and 60 %. This shows that even though there are some uncertainty in the measurements, the additional information is very valuable if the reservoir is small compared to the total inflow in the flood period.

Sammendrag

Hovedmålet til denne oppgave er å evaluere verdien av snømålinger for planleggingen av strømproduksjonen i norske vannkraftverk. Dette er undersøkt ved å implementere en approksimativ minste-kvadraters Monte Carlo metode for å finne den optimale produksjonsstrategien. Optimeringsalgoritmen bruker dynamisk programmering til å finne den optimale strategien. Strømprisen er deterministisk, mens tilsiget er stokastisk. Snømålinger er deretter inkludert i modellen for å regne ut hvilken verdi målingene kan tilføre. Realistisk data fra et stort vannkraftverk i Norge er brukt for å tilpasse en normalfordeling for å estimere tilsiget. Korrelasjonen mellom snøen og tilsiget er studert for å finne ut hvordan ulike snømengder påvirker tilsiget.

En dataanalyse viste at den maksimale snømengden og det totale tilsiget i uke 16-32 er høyest korrelert med en korrelasjonskoeffisient på 0.85. Numerisk testing av optimeringsmetoden viste at strømprisen og øvre grense av reservoaret er de to viktigste faktorene som påvirker produksjonsstrategien. Verdien av snømålingene varierer for ulike parametere i modellen. Når den øvre grense av reservoaret er stort sammenlignet med tilsiget, har ikke snømålingene noen verdi. Når reservoaret er mindre, er sjansen for oversvømmelse større og snømålingene er verdifulle når produksjonsstrategien skal optimeres. Ved å inkludere snømålingene, kan verdien øke mellom 0 og 10 % for ulike parametere i modellen. Den årlige produksjonen av vannkraft i Norge er 130TWh og er verdt rundt 4 milliarder kroner. Dette viser at selv en liten prosentvis økning kan gi en stor verdi.

Verdien til snømålingene vil synke hvis man inkluderer en viss usikkerhet i målingene. Hvis 40 % av målingene har en litt høyere eller lavere verdi enn realiteten, så vil verdien synke med 25 %. Verdien vil også synke hvis snøen og tilsiget har en lavere korrelasjonskoeffisient. Ved å bruke en korrelasjonskoeffisient lik 0.55 og 0.25 vil verdien synke med henholdsvis 24 og 60 %. Disse to resultatene viser at selv om det er en viss usikkerhet i snømålingene og korrelasjonen i dataen varierer, vil snømålingen tilføre mye verdi hvis reservoaret er lite i forhold til tilsiget.

Acknowledgment

The master's thesis was written as a completion of a master degree in Industrial Mathematics at the Norwegian University of Science and Technology. The work has been carried out at the Department of Mathematical Science during the spring semester 2016.

I would like to thank my supervisors Prof. Jo Eidsvik and Prof. Stein-Erik Fleten for all inspiration and discussion. I would like to show my gratitude for the Norwegian power company that provided historical data from one of their power plants. Acknowledgements are also directed to Dr. Oddbjørn Bruland from Sintef and Dr. Knut Sand and Mr. Yisak Sultan from Statkraft for the discussion regarding measurements and data from a catchment area in Sør-Trøndelag.

Heidi Liljeblad Ødegård, Trondheim June 2016

Contents

Figures

Tables

Chapter 1

Introduction

In Norway 95% of all the produced electricity is from hydropower. The first hydropower plant was built in 1891 (Den Norske Regjeringen, 2014). This gives Norway more than 100 years of experience with hydropower. The country is today the biggest producer of hydropower in Europe and number six worldwide. The total production in Norway was in 2014 130 TWh worth more than 4 billions NOK (SSB, 2015). In many countries, such as England, the power plants are run by using central scheduling (Fosso et al., 1999). This means that each power plant does not have to decide how to control the reservoir, but follows central guidelines. Norway has no central scheduling and optimization algorithms are used for the scheduling at each power plant separately. Because of this, there have been a lot of research on the topic and the models have become more complex and adapted to each power plant (Wallace and Fleten, 2003). The scheduling of a hydropower plant is a complex procedure with a lot of uncertain factors that can influence the decisions. The goal is to best exploit the water reservoir and produce the right amount of electricity at the right time. By using data and historical experience, the inflow from rain and melted snow can be estimated. In Norway, this inflow consists of both rainwater and melted snow from the catchment area. The snow measurements can then be included in optimization algorithms to find the best decision, but how much do the snow measurements influence the result?

By using decision theory, the importance of the snow measurements can be studied. The use of decision theory can add more knowledge about the case and substance to the decision. This

can be done by calculating the value of information(VoI). The VoI is the maximum amount of money that the decision maker should be willing to pay for the information (Eidsvik et al., 2015, p. 94). If the VoI is large, the added information clearly leads to improved scheduling. Calculating the VoI gives the opportunity to study when the measurements are important and when they are redundant.

Goals

The goals of the thesis are to:

- Implement a regression- and simulation-based method for the scheduling of a hydropower plant.
- Use the method to approximate the VoI.
- Analyze historical data and evaluate how the snow measurements and the inflow are correlated.
- Evaluate when the snow measurements are valuable

Structure of the rapport

Chapter 2 discusses the concepts of optimization, decision tree methods and the VoI. This motivation uses a small-size running example to show the different concepts used in the optimization. Chapter 3 describes the main methodological contributions, with an approximative algorithm used to calculate the scheduling for a hydropower plant, and the calculation of the VoI. Chapter 4 analyzes realistic data from a large-size Norwegian hydropower plant. It discusses the inflow, snow reservoir, production, reservoir levels and the spot prices, how these are measured and the uncertainty of the measurements. The correlation between the snow and the inflow is also studied. Chapter 5 describes the numerical testing and the results of the method, applied on the Norwegian power plant. Finally the conclusion and some ideas for further work is discussed in Chapter 6.

Chapter 2

Motivation

This is a motivating chapter, illustrating concepts for the optimization problem. This is done by using a small-size running example to explain the different stages in the process. It will discuss dynamic programming, curse of dimensionality and the calculation of VoI.

Hydropower plants consist of a dam, a turbine, a generator and transmission lines. Water from rain and melted snow are stored as potential energy in the reservoir. The turbine gets pushed by the water to spin and converts the kinetic energy in the water, to mechanical energy. The generator is connected to the turbine and converts the mechanical energy to electrical energy and transmission lines carry the power from the power plant to the households. The power plant can produce different amounts of energy depending on the size of the turbine and the velocity of the water. The amount of energy can be adjusted quickly, it takes normally 60-90 seconds from the start-up to a full production (Susskind and Raseman, 1970, p. 15). Since it is easy to change the production rate, the system is very flexible. The maximum production rate is one of the most limiting factors for a power plant. The higher amount of energy it is possible to produce, the more flexible the system is. The main components of the model are defined below:

- Time is discretized and represented by $t \in [0, T]$, where T is the finite time horizon. One time step represents one week. The running example uses two time steps, T = 2.

- The inflow q_t is a stochastic variable which describes the weekly inflow from rain and melted water. A stochastic variable like q_t, can also be called an exogenous variable. The

inflow is revealed at the start of each period. In this chapter the inflow is discretized and can take two values: $q_{t,1}$ and $q_{t,2}$. $q_{t,1}$ means that at time t the power plant has a small inflow, and $q_{t,2}$ means that it has a big inflow.

- The control variable a_t describes the amount of water that is used to electricity production at time t. The control variable can also be called an endogenous variable or decision variable. The control variable is discretized and in the running example it is used two production levels, $a_{t,1}$ and $a_{t,2}$. $a_{t,1}$ means that at time t the power plant has a low production and $a_{t,2}$ means that they have a high production.

- The water level in the reservoir at time t is represented by L_t. This is influenced by both the inflow, q, and the production, a: $L_{t+1} = L_t + q_t - a_t$.

- The reservoir has upper and lower limits L_{min} and L_{max}. If the reservoir level crosses these boundaries, the payoff will be penalized and the company will loose money.

- The spot price, c_t, is deterministic in this problem. This can be decided by using historical data. The price has yearly variations caused by seasonal variations of the supply and demand ratio.

Figure 2.1 shows an overview of the reservoir with some of the parameters. To find the optimal strategy for the production over a longer time, many different methods can be used. Common for many of the methods is the use of dynamic programming (Séguin et al., 2015).

2.1 Dynamic programming

Dynamic programming is a method to solve complex problems by dividing them into smaller subproblems that are easier to solve. The subproblems are solved only once and the solutions are stored for later use. Dynamic programming is used in many different fields, for instance computer science, economics and mathematical optimization. Many of the problems that are solved by using dynamic programming are sequential problems. A sequential problem uses only

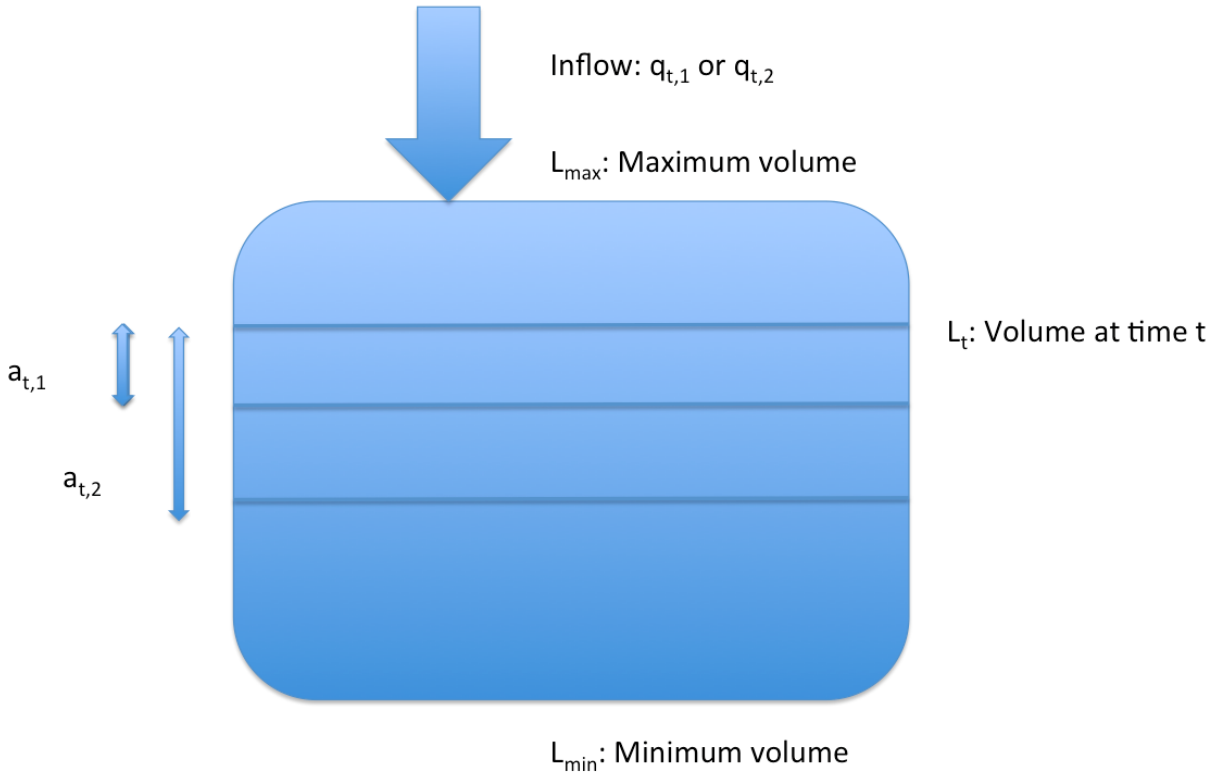

Figure 2.1: Overview of the situation with some of the variables.

the solutions from the previous subproblems to solve the current subproblem. One example of a sequential problem is the calculation of Fibonacci's sequence. One of the most common ways to visualize and solve sequential problems is the decision tree method. This is a simple, but robust method used to solve small-size problems. A decision tree is constructed for discrete state systems and shows all the different states the system can be in. An example is showed in Figure 2.2. The states are showed as circles and squares and are linked with lines that shows the transition possibilities. A circle means that the next step is stochastic, while a square means that the next step is made by a decision. The figure shows the decision tree with the different inflows, q_t and decisions, a_t written for every scenario. For every time step, there are one decision and one inflow. The value for each of the scenarios can be calculated and the optimal strategy can be found by comparing the values for the different strategies. By calculating the expected value for the different scenarios, the method finds the long-term optimal production level. This is a sequential problem, that uses dynamic programming and starts at the time horizon, T, (Sucar

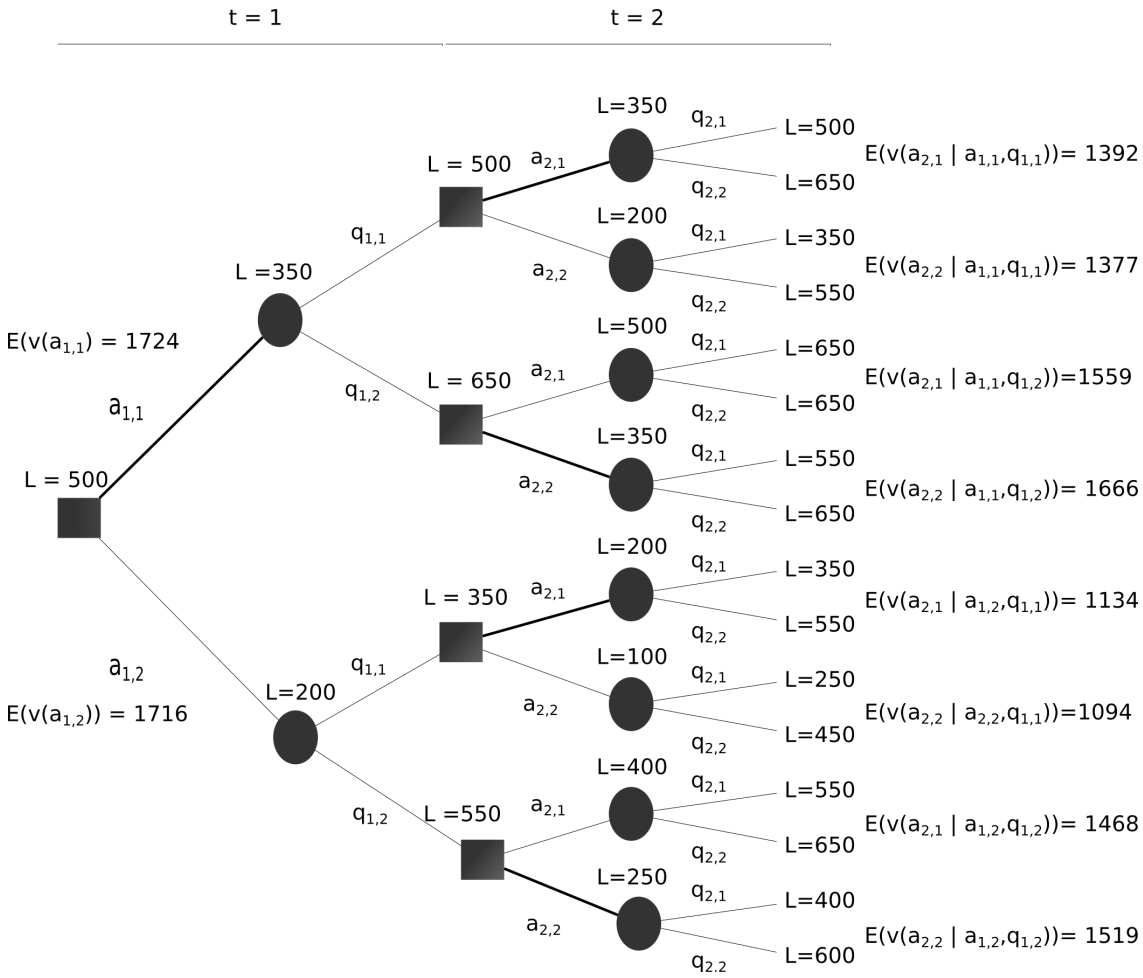

Figure 2.2: Decision tree with the expected value for each of the decisions $a_{t,1}$ and $a_{t,2}$. $a_{t,1}$ means that at time t the power plant has a low production and $a_{t,2}$ means that they have a high production. The volume of the reservoir at each node, L, is also written in the figure.

et al., 2012, p. 110). In these calculations Bellman's equation is used. Bellman's equation is also called dynamic programming equation and describes a method to calculate the optimal value by dynamic programming. It goes backwards in time and calculates the values for all the possible states at each time step. If there are no stochastic variables in the problem, Bellman's equation becomes:

$$v_t = \max_{a_t}\left[\pi(a_t) + \max_{a_{t+1}}\left(v_{t+1}(a_{t+1})|(a_t)\right)\right].$$

The formula is recursive and uses the values at step $t+1$ to decide the optimal step and the value, v_t, at time t. The values are calculated by using the immediate payoff $\pi(a_t)$ and the future payoff. The $\pi(a_t)$ is calculated by using the production rate and the spot price at time t: $\pi(a_t) =$

$a_t \cdot c_t$. The term $\max_{a_{t+1}} \left(v_{t+1}(a_{t+1}) | (a_t) \right)$ uses the values at step $t+1$ to find the long-term payoff. If there is a stochastic variable in the problem, the equation becomes:

$$v_t = \max_{a_t} \left[E\big(\pi(a_t, q_t)\big) + \max_{a_{t+1}} \Big(E\big(v_{t+1}(a_{t+1}, q_{t+1}) | (a_t, q_t)\big) \Big) \right].$$

Since the inflow is stochastic, the expected value is calculated to take all the possible inflows into account (Powell, 2011, p. 60). At time T the scenarios have different volumes L_T. To be able to compare the values of the scenarios with each other, the first step becomes a little different:

$$v_{T-1} = \max_{a_{T-1}} \Big[\pi(a_{T-1}) + \phi(L_T, c_T) \Big].$$

ϕ calculates the value of the water in the reservoir at the time horizon and can be $\phi(L_T, c_T) = L_T \cdot c_T$. This is equal to selling all the water in the reservoir at the spot price at the time T.

2.2 Description of the running example

To see how dynamic programming and decision trees work, a small-size running example will be discussed in this section. The decision tree for this case is showed in Figure 2.2 and shows the 16 different scenarios. For this case the Bellman's equation becomes

$$v_1 = \max_{a_1} \left[E(\pi(a_1, q_1)) + \max_{a_2} \Big(E(\pi(a_2, q_2) | (a_1, q_1) + E(\phi(a_1, a_2, q_1, q_2) | (a_1, q_1))) \Big) \right]. \quad (2.1)$$

The value function at the time horizon, ϕ, is chosen to be $\phi(L_T, c_T) = L_T \cdot c_T$. Since the method goes backwards, the value for the second time step is calculated first:

$$v_2(a_1, q_1) = \max_{a_2} \Big[\sum_{q_2=1}^{2} \pi(a_2, q_2) P(q_2|q_1) + \sum_{q_2=1}^{2} \phi(a_1, a_2, q_1, q_2) \cdot P(q_2|q_1) \Big]. \quad (2.2)$$

At this time step, there are four possible states and four values that have to be calculated, $v(a_t, q_t)$. By using Equation (2.1) and (2.2), the value v_1 can be solved recursively by the formula:

$$\begin{aligned} v_1 &= \max_{a_1}\Big[E_{q_1}(\pi(a_1,q_1)) + E_{q_1}(v_2(a_1,q_1))\Big] \\ &= \max_{a_1}\Big[E_{q_1}(\pi(a_1=1,q_1)) + E_{q_1}(v_2(a_1=1,q_1)), E_{q_1}(\pi(a_1=2,q_1)) + E_{q_1}(v_2(a_1=2,q_1))\Big] \end{aligned} \quad (2.3)$$

In the calculations the probability distributions of the inflows are used. The inflow has a marginal distribution which describes the probability of the first inflow: $P(q_1) = [p_1, 1-p_1]$. A transition matrix is also used in the calculation to include the dependencies between the inflow at two time steps:

$$P(q_{t+1}|q_t) = \begin{array}{c} \\ q_{t,1} \\ q_{t,2} \end{array} \begin{array}{c} \begin{array}{cc} q_{t+1,1} & q_{t+1,2} \end{array} \\ \begin{pmatrix} p_{11} & 1-p_{11} \\ 1-p_{22} & p_{22} \end{pmatrix} \end{array}.$$

If the inflow at time step t is small, $q_{t,1}$, then there is a probability of p_{11} that next inflow is small and a probability of $1-p_{11}$ that next inflow is big. When all the values are calculated the optimal strategy β can easily be found. An example of this is showed in Figure 2.2, where the optimal decision at each step is marked with a thicker line. This can be found by comparing the expected values written in the figure.

The implementation of the method was done by using MATLAB, (MATLAB, 2016). A lot of numerical testing with different parameters were done to explore which parameters that influenced the most. To begin with the optimal strategy were tested by changing the parameters c, a, q, L_0, L_{min} and L_{max}. The testing showed that the reservoir limits play an important role in the problem. If the reservoir is big compared to the starting volume and the inflow, the optimal decision is made only based on the price. Then the production is high when the price is high and low when the price is low. When the reservoir is smaller, the chance of overflow is bigger. Because of this, the decision is no longer only decided based on the price, but also to avoid the boundaries. If the price varies a lot, then it is more important to sell at the highest price, than to

avoid overflow. The choice of the production rates, $a_{t,1}$ and $a_{t,2}$, and the inflow levels, $q_{t,1}$ and $q_{t,2}$ can also influence the optimal strategy, but are not as important as the reservoir level and the spot price.

In the running example the goal is to see whether the snow measurements can add any value to the problem, so before any decision is made, the snow is measured. This additional information is denoted y. To keep it simple the information, y, can have tree different values $\{1,2,3\}$, representing the different snow levels $\{low, medium, high\}$. In this case the transition probabilities are changed because of the measurements. Instead of the marginal distribution $P(q_1)$, the conditional distribution $P(q_1|y)$ is used. Then, the probability for the inflow changes, based on the snow measurements. If the snow is measured to be low, there will be a higher probability for a small inflow. The transition matrix $P(q_2|q_1)$, is also replaced by the conditional distribution $P(q_2|q_1, y)$. By using the additional information and the conditional distributions, the VoI can be calculated.

2.3 Prior Value, Posterior Value and Value of Information

By using the decision tree method to find the optimal strategy and the value of this strategy, it is possible to describe the value of the snow measurements. One method to find this value is to calculate the VoI (Eidsvik et al., 2015, p. 95). If the VoI is high, the additional information adds much value to the problem, and results in a better solution than the optimal strategy found without additional information. If the VoI is low, on the other hand, the additional information is not so valuable. The VoI is calculated by using the prior value(PV) and the posterior value(PoV).

Prior Value

The PV is the value of the decision situation without information. The PV describes the value of the optimal strategy β and is described by the formula below:

$$PV = E(v(q, \beta))$$

v calculates the value for inflow q and strategy the optimal β. The expected value can be calculated with the formula

$$E(v(q,\beta)) = \sum_{q} v(q,\beta) \cdot p(q).$$

The $p(q)$ is the possibility for the inflow $q = [q_1, q_2]$. This will be a product of the marginal distribution and the transition matrix. This is done by using Bayes' rule (Eidsvik et al., 2015, p. 40). Bayes' rule can be written as below, (Walpole et al., 2012, p. 72):

$$p(x,y) = p(y|x) \cdot (x) \tag{2.4}$$

The prior value for the running example, is the same as the calculated v_1 described in Equation (2.3).

Posterior Value

The PoV describes the value of the decision problem using the measured data y. The conditional distributions are used in the calculation of the PoV:

$$PoV = \sum_{y} \max_{i} (E(v(q|y,\beta_i))p(q|y).$$

Here, the β_i is the optimal strategy for snow measurement i. For the running example, the formula for the PoV becomes

$$PoV = \max_{a_1} \left[E(v(a_1,q_1|y)) + \max_{a_2} \left(E(v(a_2,q_2)|(a_1,q_1,y) + E(\phi(a_1,a_2,q_1,q_2)|(a_1,q_1,y))) \right) \right] \tag{2.5}$$

The expected value is calculated by using the following formula:

$$E(v(a_1,q_1|y)) = v(a_1,q_1=1|y)P(q_1=1|y) + v(a_1,q_1=2|y)P(q_1=2|y).$$

The second term in Equation (2.5) can be called PoV_2 be written as

$$PoV_2(a_1,q_1) = \max_{a_2} \left[\sum_{q_2=1}^{2} v(a_2,q_2|y)P(q_2|q_1,y) + \sum_{q_2=1}^{2} \phi(a_1,a_2,q_1,q_2) \cdot P(q_2|q_1,y) \right].$$

By using recursion the formula for the PoV becomes

$$\begin{aligned} PoV &= \max_{a_1}\Big[E_{q_1}(v(a_1,q_1|y)) + E_{q_1}(PoV_2(a_1,q_1|y))\Big] \\ &= \max\Big[E_{q_1}(v(a_1=1,q_1|y)) + E_{q_1}(PoV_2(a_1=1,q_1|y)), E_{q_1}(v(a_1=2,q_1|y)) + E_{q_1}(\beta_2(a_1=2,q_1|y))\Big]. \end{aligned}$$

If the inflow scenarios are fully known, the perfect information $PoV_{perfect}$ can be calculated. In reality this never happens, but it is a good measure on how much it is possible to earn. If the $PoV_{perfect}$ is much higher than the PoV, there is a lot of potential in the optimization process. The formula for $PoV_{perfect}$ is:

$$PoV_{perfect} = \int \max_i (E(v(q,\beta_i))p(q)dq.$$

Value of Information

The VoI can then be calculated by using the formula:

$$VoI = PoV - PV. \tag{2.6}$$

The VoI describes the value of the additional measurements. By calculating the VoI it is possible to decide whether the information should be included in the model or not. If the price to measure the data, y, is lower than the VoI, it is valuable for the company to include the measurements in the model.

Some numerical testing were done by using three classes of snow measurements $\{low, medium, high\}$. To calculate the PoV, the distributions $P(q_{t+1}|q_t)$, $P(y|q_1,q_2)$ and $P(q_t)$ were used. These three probability distributions were used to calculate the distributions used in the calculations of the PoV: $P(q_{t+1}|q_t,y)$, $P(q_t|y)$ and $P(y)$. This is done by using Bayes' rule, Equation (2.4). Many different distributions were tested. This was done because the dependence between the snow

and the inflow is uncertain and can variate from power plant to power plant. The conditional distributions below were used in one of the experiments:

$$P(q_{t+1}|q_t) = \begin{array}{c} \\ q_{t,1} \\ q_{t,2} \end{array} \begin{array}{c} \begin{array}{cc} q_{t+1,1} & q_{t+1,2} \end{array} \\ \begin{pmatrix} 0.7 & 0.3 \\ 0.3 & 0.7 \end{pmatrix} \end{array}.$$

$$P(y|q_1,q_2) = \begin{array}{c} \\ 11 \\ 12 \\ 21 \\ 22 \end{array} \begin{array}{c} \begin{array}{ccc} y=1 & y=2 & y=3 \end{array} \\ \begin{pmatrix} 0.99 & 0.005 & 0.005 \\ 0.05 & 0.9 & 0.05 \\ 0.05 & 0.9 & 0.05 \\ 0.005 & 0.005 & 0.99 \end{pmatrix} \end{array}$$

$$P(q_t) = \begin{array}{c} \begin{array}{cc} q_{t,2} & q_{t,2} \end{array} \\ \begin{pmatrix} 0.5 & 0.5 \end{pmatrix} \end{array}$$

$P(y|q_1,q_2)$ says a lot about the dependencies between the inflow and the snow measurements. The numbers 11, 12, 21 and 22 tell which two inflows that have been seen at time t and $t+1$. If there have been two small inflows the probability for a small snow reservoir is 0.99. The spot price and the reservoir level were chosen such that the decision is based on both avoiding the limits and the spot price. This resulted in that different snow measurements resulted in different strategies, showed in Table 2.1. $\beta(1,2)$ in the table, means that the first decision is to lower the small amount and then a big inflow is observed. From the different optimal strategies, it is possible to see that much snow in the catchment area will result in a higher production even though the price is lower. This is done to avoid overflow and shows that the long-term optimal strategy not always is optimal at every step separately. For the case with a little snow in the catchment area, the power plant will have a small production if the inflow is small and a big production if the inflow is big. The snow measurements make the power plant change production strategy

Table 2.1: The different optimal strategies and the correspondent expected values for the prior value(PV) and the three different values of y.

	PV		PoV(y=1)		PoV(y=2)		PoV(y=3)	
	decision	value	decision	value	decision	value	decision	value
β_1	1	1824	1	1530	1	1854	2	2165
$\beta_2(1,1)$	2	1485	1	1322	2	1705	2	1664
$\beta_2(1,2)$	2	1774	2	1640	1	1613	2	1898
$\beta_2(2,1)$	1	1188	1	1022	1	1408	1	1367
$\beta_2(2,2)$	2	1627	2	1448	1	1412	2	1793

which result in a higher revenue and a positive VoI.

The numerical values in this example are not very interesting themselves, because of the simplifications. It is however very interesting to study the structure and dependencies in the problem. Many of these things will be the same for a more realistic case. To be able to use the theory on a real hydropower plant, there have to be many more time steps. The decision tree method will then suffer from the curse of dimensionality and become too slow. This is because the number of scenarios is $(2 \cdot 2)^T$, if there are two lowering- and two inflow possibilities. The problem has an exponential run-time and when the T gets big, the method becomes too slow. An approximate method can then be used to solve the problem. Chapter 3 will explain how one of these approximative methods works for a more realistic version of this case.

Chapter 3

Method

An approximative method is presented in this chapter and will be tested on a realistic case in Chapter 5.

The method used to study the VoI for snow measurements, can be divided into two parts. The first part is to find the optimal strategy and the second part is to calculate the VoI. The first problem have to be solved by approximative dynamic programming. There are many different approximated methods that are possible to use on the optimization problem. The different methods have different approaches that makes them fit different problems. By studying the structure and the parameters of the problem, it is easier to decide which methods that will solve the problem best. In this case the problem consist of a stochastic part, q, a decision variable, a and a multiple continuous variables. After studying different optimization methods, a Least-Square Monte Carlo(LSMC) method is chosen to approximate the problem. The method is based on the one described in (Denault et al., 2013). It uses regression and simulations to optimize the control of the hydropower plant. Since the case in (Denault et al., 2013) is not identical with the case discussed here, some adjustments are made. In (Denault et al., 2013) the spot price is used as a stochastic parameter and the inflow is deterministic. In the case described here, the spot price is deterministic and the inflow is stochastic. The LSMC method is explained in Section 3.1, while the calculation of the VoI is described in Section 3.2.

3.1 Finding the optimal strategy

This method uses dynamic programming like the example in Chapter 2. Some parts of the method are very similar to the decision tree method described earlier. The algorithm starts at the time horizon, T. It uses K scenarios that each have a simulated inflow at each time step. The volume in the reservoir at the time horizon, L_T is randomly distributed between the limits of the reservoir, L_{min} and L_{max}. The value of the water at the time horizon is calculated to be $V_T = L_T \cdot c_T$. This means that the value at the time horizon equals to sell all the water that is left at time T to the spot price at the time, c_T. The method then takes steps backwards in time until it reaches the first time step. Even though the method goes backwards in time it uses forward optimization. To look closer at this procedure, one step is explained in detail.

Regression and value approximation

For scenario k and time $t+1$, the water level $L_{t+1}^{(k)}$ is known as well as the value of that scenario $V_{t+1}^{(k)}$. The value $V_{t+1}^{(k)}$ represents the value of going from reservoir level L_{t+1} at time $t+1$ to the time horizon T, by having the inflow scenarios $q^{(k)}$ and making the optimal decisions $\alpha^{(k)}$. All the decisions $\alpha_{t'}$, $t' \leq t+1$ are known from earlier time steps. α is the optimal path that is already found by moving from the time limit, T to the time t. Then at time $t+1$, the method takes a step backwards in time. This step gives two new volumes $L_{t,1}$ and $L_{t,2}$ obtained by production levels $a_{t,1}$ and $a_{t,2}$, seeing inflow q_t and ending up in L_{t+1}. They are calculated by the formulas:

$$L_{t,1} = L_{t+1} + a_{t,1} - q_t$$
$$L_{t,2} = L_{t+1} + a_{t,2} - q_t.$$

This backward step is illustrated in Figure 3.1. Then the value of the two scenarios can be calculated by the following equation:

$$V_t(q_t, a_t, L_t, c_t) = \pi(a_t; q_t, c_t) + V_{t+1}(L_{t+1}). \tag{3.1}$$

This is a sum of the payoff of producing electricity and the long-term value of going to reservoir level L_{t+1}. Figure 3.2 shows the forward step with the calculated values. Since the reservoir

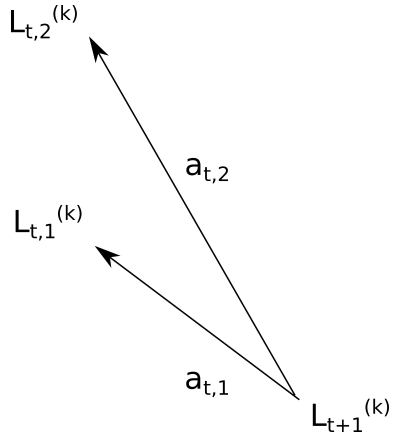

Figure 3.1: One step is taken backwards in time by using the two possible lowering possibilities $a_{t,1}$ and $a_{t,2}$.

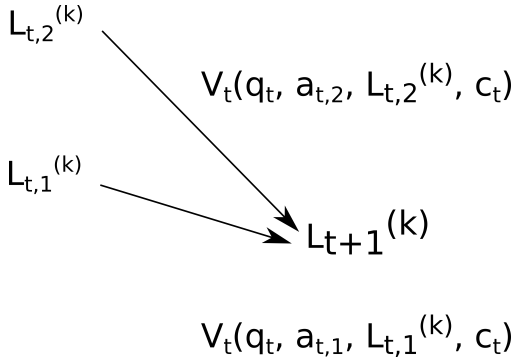

Figure 3.2: The two different states ending up in L_{t+1} and the values associated with them, calculated from (3.1).

levels at time t are different: $L_{t,1} \neq L_{t,2}$, the values of the two scenarios: $V_t(q_t, a_{t,2}, L_{t,2}, c_t)$ and $V_t(q_t, a_{t,1}, L_{t,1}, c_t)$ can not be compared directly. To find the optimal strategy, forward optimization is used. To make this forward step, both of the production levels are used from the two different reservoir levels at time t: $L_{t,1}$ and $L_{t,2}$. This forward step is showed in Figure 3.3. The long-term values are not known for the scenarios that ends up in L'_{t+1}, so the values $V_t(q_t, a_{t,2}, L_{t,1}, c_t)$ and $V_t(q_t, a_{t,1}, L_{t,2}, c_t)$ are unknown. To be able to compare the different choices, an estimation of these values have to be done. This method uses regression surfaces for this estimation. Two regression surfaces are fitted to the data, one for each of the production possibility. For decision $a_{t,1}$, the regression surface is calculated by regressing

$$\pi_t\left(a_{t,1}, q_t^{(k)}, L_{t,1}^{(k)}\right) + V_{t+1}\left(q_{t+1}^{(k)}, L_{t+1}^{(k)}\right) \quad on \quad \left(S_t^{(k)}\right).$$

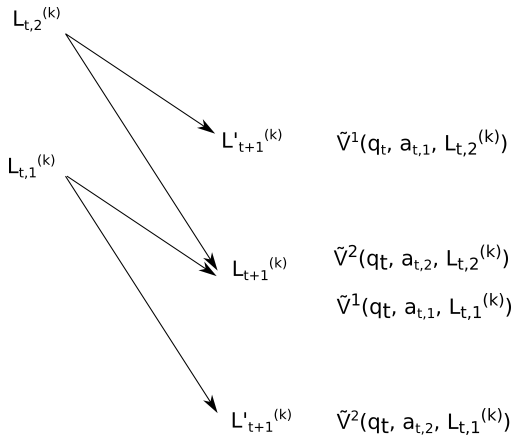

Figure 3.3: One step is taken backwards in time by using the two possible lowering possibilities $a_{t,1}$ and $a_{t,2}$.

This gives the surface called $\tilde{V}_t^1$. This surface is used to find the value of making decision $a_{t,1}$ by standing at any given point (L,q) in the feasible area. Similarly the regression surface, $\tilde{V}_t^2$, is calculated for the decision $a_{t,2}$, by regressing

$$\pi_t\left(a_{t,2}, q_t^{(k)}, L_{t,2}^{(k)}\right) + V_{t+1}\left(q_{t+1}^{(k)}, L_{t+1}^{(k)}\right) \quad on \quad \left(S_t^{(k)}\right).$$

Figure 3.4 shows the two regression surfaces separately for one time-step. By comparing them, it is hard to see a difference. Since the production and inflow are much lower than the reservoir level, the difference between the two decisions are small. The regression surfaces can now be

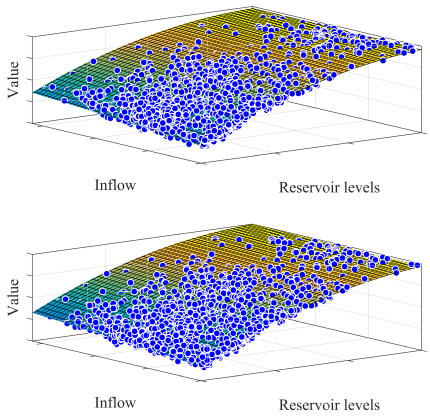

Figure 3.4: The regression surfaces are shown from the side, one for lowering a small volume and one for lowering a big volume. The blue circles represent the K scenarios.

used to estimate the value of the two different production rate for any point in the Lq-plane. All

the four values showed in Figure 3.3 are found by using the two regression surfaces. This makes it possible to compare the different decisions and find the optimal strategy.

Figure 3.5 shows the regression surfaces from above with all the K scenarios. All the points $(L_{t,1}, q_t)$ and $(L_{t,2}, q_t)$ are plotted by using two different colors. The black circles show the small production and the red ones the big production. The two background colors represent the regression surface that is highest at this point. This corresponds to which of the production rates that gives the highest payoff. The white is to produce the smallest amount $a_{t,1}$, while the grey is to produce the biggest amount $a_{t,2}$.

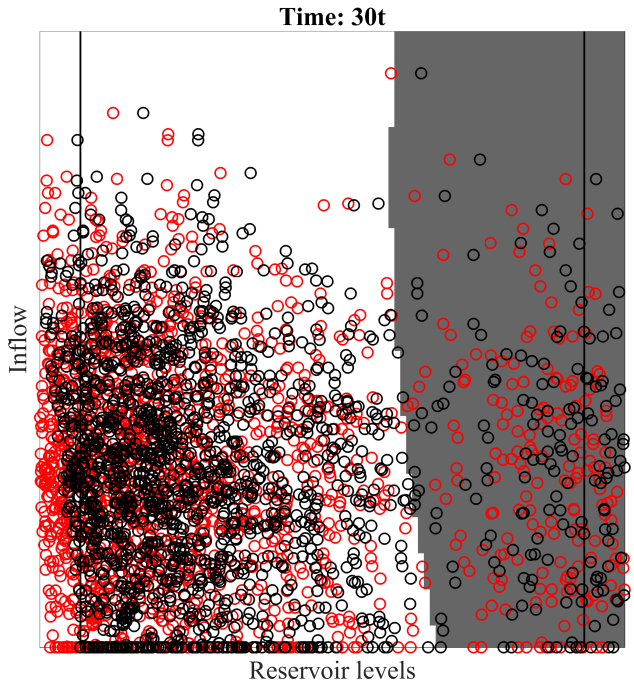

Figure 3.5: The regression surfaces are shown from above. The white area represent the domain where decision $a_{t,1}$ is the optimal solution and the grey area where $a_{t,2}$ is the optimal action.The circles represent the K scenarios after producing $a_{t,1}$ in black and $a_{t,2}$ in red.

To decide the optimal decisions, the values of lowering $a_{t,1}$ and $a_{t,2}$ are calculated for the point $(L_{t,1}, q_t)$. The values are compared and the optimal decision for that case is decided: $\alpha(L_{t,1}) = \text{argmax}_{1,2}(\tilde{V}_t^1(L_{t,1}), \tilde{V}_t^2(L_{t,1}))$. Similarly, this is done for volume $L_{t,2}$ and the optimal value $\alpha(L_{t,2})$ is found. Since both the inflow and the lowering possibilities are much smaller than the reser-

voir capacity $L_{max} - L_{min}$, the two points $(L_{t,1}, q_t)$ and $(L_{t,2}, q_t)$ will lie close to each other. The two optimal decisions $\alpha(L_{t,1})$ and $\alpha(L_{t,2})$ will be different only if the points lie on each side of the border between the white and grey area in Figure 3.5. This happens very few times and special decisions have to be made in these cases. For most cases the two points will have the same background color. Then $\alpha(L_{t,1}) = \alpha(L_{t,2})$ and the optimal decision is the one that ends up in L_{t+1}. Figure 3.3 shows the situation where the optimal strategy is marked with a thicker line. Here $\alpha(L_{t,1}) = \alpha(L_{t,2}) = a_{t,2}$, so the optimal decision is $a_{t,2}$. The reservoir level at time t becomes $L_{t,2}$ since this is the volume that ends up in L_{t+1} by lowering $a_{t,2}$. If the decisions are not the same, $\alpha(L_{t,1}) \neq \alpha(L_{t,2})$, the strategy is decided randomly, where both of the possibilities are equally probable. In order to be sure that there are no clustering and leakage from the feasible are, some additional restrictions are made.

Clustering and Leakage

In a method that goes forward, the scenarios tend to lead away from the reservoir limits, L_{min} and L_{max} (Denault et al., 2013). This is done to avoid overfilling or reaching the bottom of the reservoir. If the reservoir is close to the upper limit at time t, it will be lowered with the maximum amount possible to prevent that the inflow will cause overflow at the next step. In a method that moves backwards and uses forward optimization, the opposite happens. So going from $t+1$ to t the optimal choice is $a_{t,2}$, the the reservoir level becomes $L_{t,2}$ which is greater than $L_{t,1}$. Then the method ends up closer to the upper limit than what it could have done. This makes the scenarios move towards the limits, when going backwards in time. To avoid this problem there are upper and lower limits of the reservoir where the payoff function is penalized. This penalty function is simple and linear and the payoff becomes

$$\pi(a_t; q_t, L_{t+1}, c_t) = \begin{cases} c_t \cdot a_t & \text{if } L_{min} < L_t < L_{max} \\ c_t \cdot (L_{t+1} + a_t - L_{min}) & \text{if } L_t < L_{min} \\ c_t \cdot (L_{max} - L_{t+1} - a_t) & \text{if } L_t > L_{max} \end{cases} \tag{3.2}$$

This means that if the water level moves beyond the limits L_{max} and L_{min}, the power plant will produce extra electricity without getting any payoff. Because of the penalized payoff function,

the method will more often make a decision that leads away from the limits. Different penalty functions, such as quadratic penalty, were tested in the method without giving any significant changes. The linear penalty function in Equation (3.2) is therefor used in the method to keep it simple and solid.

The penalty alone is not always enough to keep the scenarios in the area between L_{min} and L_{max}. To prevent scenarios to leak out of the feasible area, two new limits are added: L^-_{min} and L^+_{max}. These limits are more extreme than the existing limits. Scenarios that go beyond these limits are randomly reassigned to a level in the feasible area. This is done to avoid clustering around the limits and leakage from the feasible area. If a big percentage of the scenarios are placed in the same area, the regression-process can be inaccurate. This is because the base of the regression surfaces becomes limited and only covers a small bit of the domain. By reassigning the scenarios that cross L^-_{min} and L^+_{max} to the feasible area, the method stays more stable and accurate. The percentage of scenarios that cross the outer limits should not be very high. If $L^+_{max} = L_{max} + a_{t,2}$ and $L^+_{min} = L_{min} - a_{t,2}$, then there are in average around 5 % that are replaced. This is low enough to make the method function well.

Number of lowering possibilities

The method is described with two lowering possibilities to make it easier to explain and understand how the method works. It is possible to include more lowering possibilities, which will make the optimal strategy more flexible and better adjusted to the price. This does not change the implementation of the method very much, but expands some of the parts that are already implemented. If there are four different lowering possibilities, there will be four different regression surfaces and four values that have to be compared to find the optimal strategy.

Calculations of the forward strategy

The method is optimizing the strategy for the K scenarios. These can be used to find a forward strategy for an initial volume L_0. This is done by using the k nearest neighbors of the point (L, q). If the number of scenarios K is big enough, there will be k neighbors lying relatively close

to the point (L_t, q_t). The distances are checked to make sure that the k nearest neighbors lie close enough. Then the decisions of all the neighbors can be used to find the optimal decision. Mathematically, this is showed in the formula below:

$$\beta_t(V_t, q_t) = \text{round}\Big(\frac{1}{k}\sum_{i=0}^{k} \alpha(V_t^{(i)}, q_t^{(i)})\Big).$$

The points $(V_t^{(i)}, q_t^{(i)})$ for $i = 1 : k$ represent the k nearest neighbors. $\alpha(V_t^{(i)}, q_t^{(i)})$ is the optimal decision for point $(V_t^{(i)}, q_t^{(i)})$. An example of finding the optimal strategy β is illustrated in figure 3.6. The blue circle is the current position on the Lq-plane and the big circle defines the k nearest neighbors. The red circles represent the scenarios where the optimal strategy is a big production, $a_{t,2}$ and the black circles represent the scenarios where the optimal strategy is small production, $a_{t,1}$. The optimal decision of the blue circle is a big production because it is more red circles than black ones.

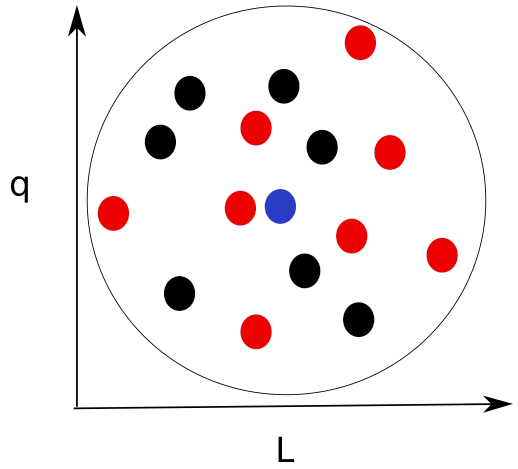

Figure 3.6: The blue circle is the current position in the Lq-plane, and the circle defines the 15 nearest neighbors of the blue circle. The red ones have an optimal decision of producing a big amount of electricity, while the black one have an optimal decision of producing a small amount of electricity.

To summarize the calculation of the optimal strategy, Algorithm 1 is provided.

Deciding the initial volume L_0, time horizon T and lowering possibilities a_t;
Generate K stochastic inflows q;
Randomly generate the reservoir levels between L_{min} and L_{max} for time T;
Compute the values at time T;
for $t = T$ **to** $t = 0$ **do**
  Compute the regression surfaces $\widetilde{V}^a(q, L)$, $a \in \{1, 2\}$;
  For each $2K$ levels compute the most valuable decision: $L_t^{(k)}$;
  Associate a level $L_t^{(k)}$ for each strategy, k, according to the results in the above step;
  Find value $\widetilde{V_t}(q_t, L_t)$ by using the regression surfaces;
end
Compute the value for the initial volume L_0 by using the regression surfaces at time 0;

Algorithm 1: An optimization algorithm that uses regression and simulation to calculate the scheduling of the hydropower plant

3.2 Value of Information

As described in Section 2.3, the VoI is the difference between the value calculated with the additional information and without. The value is calculated by using the optimal strategy β and an initial volume V_0. Starting at the first time step, the strategy β is used and the values are calculated. Since it is the flood period at the spring that is of special interest, the calculations stop at week 20. Then the value of the water in the reservoir is added as the volume times the mean spot price from time step 20 until the time horizon. This is done to avoid impact from different scheduling in the future and the burn in period. The formula for the value becomes:

$$\eta(V_0, q^l, \beta_i)\big) = \pi(\alpha(\beta_i), c_t, q^l) + V_{20} \cdot \bar{c}.$$

The function π is the penalized payoff function, in Equation (3.2).

The calculations of the PoV can be done in many different ways. The additional information, y, can be included differently. Which way that is optimal for each problem have to be decided by looking at historical data. If there are much information about the snow and the inflow, a likelihood function is the best choice $P(q|y)$. Often, there is not enough information to fit a model like this and uncertainty in the measurements can make the method too precise to function in a realistic case. Instead of a likelihood it is possible to use a rougher classification for the snow

measurements. Then the snow information y can be divided into Y classes, each with an equal probability to happen: $p(i) = \frac{1}{Y}$, $i = 1 : Y$. Since the snow influences the inflow, the K inflow scenarios are also divided into Y classes. How the division is done depends on the data and how the snow and the inflow are correlated. One example of how this is done is discussed in Chapter 4. β_i is the optimal strategy for information i, $i = 1 : Y$ and q^l is the inflow scenarios in class l, $l = 1 : Y$. By calculating the PoV and the PV, the VoI can be calculated by using Equation (2.6). The PoV for one particular class $i \in Y$, is calculated for an initial volume V_0 by the formula:

$$PoV_i(V_0) = \max_{l=1:Y} \big(\eta(V_0, q^l, \beta_i)\big).$$

The equation calculates the maximum of the value over the different inflow classes $q^l, l = 1 : Y$. This is done for each of the different strategies $\beta_i, i = 1 : Y$. Finally, the PoV can be calculated by

$$PoV(V_0) = \sum_{i=1}^{Y} PoV_i(V_0) \cdot P(i). \tag{3.3}$$

The PV can be calculated in different ways. To make the calculation of the PV and the PoV consistent, double expectation, $E(V) = E(E(V|y))$, is used to calculate the PV. The formula for the PV becomes:

$$PV(V_0) = \max_{l=1:Y} \Big(\sum_{i=1}^{Y} P(i) \cdot \big(\eta(V_0, q^l, \beta_i)\big) \Big). \tag{3.4}$$

This is calculated in a similar way as the PoV, but the order of the maximization and the summation is changed. This means that for every inflow q^l, the value is calculated for all the Y different strategies β. By using the same inflow scenarios in both of the calculations the $VoI = PoV - PV$ is guaranteed to be positive or zero. To easier understand the calculations, the different values used in Equation (3.3) and (3.4) are shown in Table 3.1. In this example there are three classes, $Y = 3$.

Algorithm 2 shows an overview of the calculation of the VoI.

Table 3.1: The values used in the calculations of the PV and the PoV. q^1 is the inflow scenarios when $y = 1$, and β_1 is the optimal strategy when $y = 1$. The function η calculates the value of using path β and inflow q by starting with an initial reservoir level L_0.

	q_1	q_2	q_3
β_1	$\eta(V_0, q^1, \beta_1)$	$\eta(V_0, q^2, \beta_1)$	$\eta(V_0, q^3, \beta_1)$
β_2	$\eta(V_0, q^1, \beta_2)$	$\eta(V_0, q^2, \beta_2)$	$\eta(V_0, q^3, \beta_2)$
β_3	$\eta(V_0, q^1, \beta_3)$	$\eta(V_0, q^2, \beta_3)$	$\eta(V_0, q^3, \beta_3)$

Initialize the number of scenarios K and the number of classes Y;
Deciding the lowering possibilities a;
for $i = 1$ **to** Y **do**
  calculate optimal strategy β_y with Algorithm 1
end
Calculate $PV(V_0) = \max_{l=1:Y} \left(\sum_{u=1}^{Y} P(y) \cdot \left(\text{value}(V_0, q^l, \beta_y)\right) \right)$;
Calculate $PoV(V_0) = \sum_{u=1}^{Y} P(y) \cdot \left(\max_{l=1:Y} \left(\text{value}(V_0, q^l, \beta_y)\right) \right)$;
Calculate the VoI = PoV - PV;

Algorithm 2: By using different snow measurements, the Value of Information is calculated. Algorithm 1 is written in the end of Section 3.1

Chapter 4

Data

This chapter will look on the parameters in the model, how they can be measured and their uncertainty. In Section 4.1, 4.2 and 4.3 the spot price, reservoir levels and production are discussed. These are not the core parameters in the model, but are discussed initially to give basis knowledge about the parameters and the field. The most important part of the chapter is the study of the snow, inflow and how these are correlated. The snow reservoir is discussed in Section 4.4 and the inflow is discussed in Section 4.5. Here, a normal distribution is fitted the inflow, making it straightforward to simulate the K inflow scenarios. The correlation between the snow and the inflow is discussed in Section 4.6.

For each parameter an analysis of realistic data will be done. The data is from a large-size hydropower plant in Norway. The data presented is the aggregated data from multiple reservoirs. The measurements are taken every week from 2002 to 2012. The data is not complete, which can be noticed in some of the figures. Since it is the spring period that is most interesting, the data is presented from week 16 to week 15 the next year. The company and the numerical values of the data are anonymized because of confidentiality.

4.1 Spot price

The spot price is decided daily at noon and is applicable from midnight and the next 24 hours (Fosso et al., 1999). It depends on many factors, for example the supply and demand of power

and financial trends. The spot price for the period 2002-2012 is showed in Figure 4.1. The black lines represent the spot price each year and the red line is the average price. The changes from day to day are normally small and the correlation from day to day is big,(Nilsson, 2014). There are also yearly variations (Nilsson, 2014) created from different supply and demand through the year. The prices are higher in the winter when the demand is high and the supply low and lower in the summer when the demand is low and the supply high. This can also be viewed in Figure 4.1.

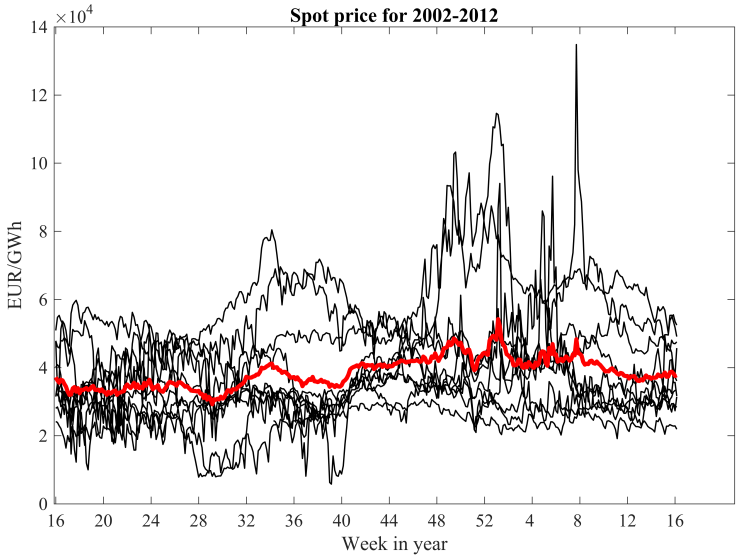

Figure 4.1: The spot prices for the years 2002-2012 are plotted in black, while the mean is plotted in red.

4.2 Reservoir levels

The amount of water in the reservoir can be found by measuring the height of the reservoir and then use the form of the reservoir to calculate the volume or energy equivalent. This can be done by using a height-volume curve that describes the volume for the different heights of the reservoirs. This was done manually before, but in the last 20 years the measuring has gradually become more digital. Today most of the power plants use digital measurements. The most usual way to measure the reservoir level digitally is by using a radar. The measuring process have multiple factors that can make the measurements incorrect. Some of these factors are:

wind, ice, temperature and changes in the weather (Raghavendra, 2013).

At the Norwegian power plant, the reservoir height are measured by using pressure cells. The volume is then found by use of a height-volume curve. The uncertainty is mainly from the transition from height to volume and is estimated to be under 5 %[1]. The reservoir levels for the Norwegian power plant are plotted in Figure 4.2. The measurements are mainly done automatically and are considered to be precise. The error is estimated to be smaller than 5%. The figure shows that the reservoir is close to the bottom before the flood period and reaches its maximum around week 44. This is in October and caused by rainwater from the autumn flood. From week 32 to 44 it is not very much rainfall because of the dryer periods in the summer, but the reservoir is still increasing. This can be because of some delay in the inflow from the melting water. This can happen if the groundwater level is low before the melting period and some of the water is used to fill up the groundwater reservoir. The ground consists of an area at the bottom that is saturated, and above this there will be an area that is unsaturated. Some of the melting water can therefor be used to fill up the groundwater. If the ground is steep the inflow from melting water will result in a river that moves fast. If there is a flatter landscape with soil, the inflow will be more even. In that case there will be a slower flow and more of the water will be used to fill up the groundwater. The groundwater will reach its minimum before the melting period, so some of the water from the groundwater will eventually flow down in the reservoir (NVE, 2016). This process depends on the geology in the area and what kind of ground there is. Power plants are often placed in areas with a steep landscape, because the potential energy is higher here. These areas are often in the mountains or fjords, with mainly rock formations. In this case, this will not be an important reason for the error, but it can influence the inflow in a smaller degree[2].

As Figure 4.2 shows the yearly variations are quite big. One year the reservoir levels are quite low all year, which indicates a very dry year with little rain and snow. Other years there are clearly very much rain and snow, resulting in the reservoir to reach its maximum. The reservoir has only had an overflow six times in the time period 2002-2012.

[1] Based on communication with an expert from the relevant power plant.
[2] Based on communication with an expert from the relevant power plant.

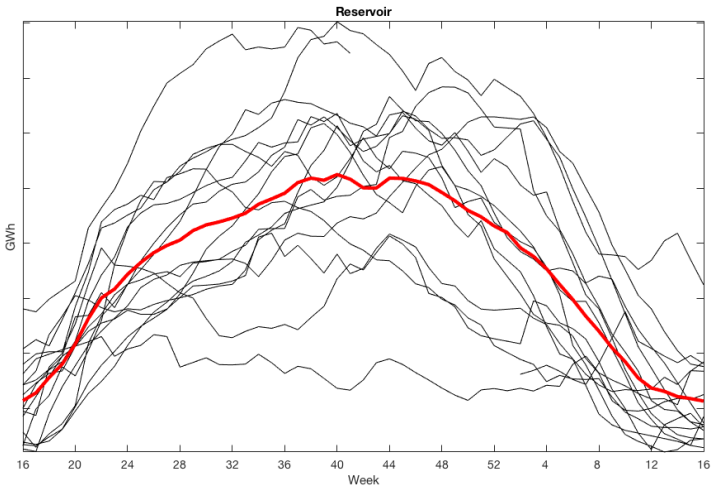

Figure 4.2: The reservoir levels for the years 2002-2012 are plotted as black curves. The mean is plotted as a red curve. The plot shows weekly measurements.

4.3 Production

How much electricity that is produced each hour is decided by the power plant. The production rate is decided, but the amount of water is also measured by looking at the velocity of the water through the turbine. This is done continuously and the measurements are quite precise. The production rates for the discussed power plant are plotted in Figure 4.3. The curves for each year is smoothened by using a moving average:

$$a_i = \begin{cases} \frac{1}{n+i}\sum_{j=-i}^{n} a_{i+j}\,, i < n \\ \frac{1}{2n}\sum_{j=-n}^{n} a_{i+j}\,, n < i < N-n \\ \frac{1}{n+N-i}\sum_{j=-n}^{N} a_{i+j}\,, x > N-n \end{cases} .$$

$$for\, i \in [1, N].$$

The N is the total number of years, while the n describes the degree of smoothening. The higher n is, the more smoothened the production gets. In the original data there is much variation every week which makes it hard to see the different years separately. The smoothened curve is plotted to make it easier to see the trends each year. The plot shows that the production is highest at the winter, emptying the reservoir before the spring flood. This is when the prices

and the demand of energy are highest Statkraft (2015). In week 16-32 while the inflow is still big, the production is not very high. This is because at this time of the year, the prices are lower. It

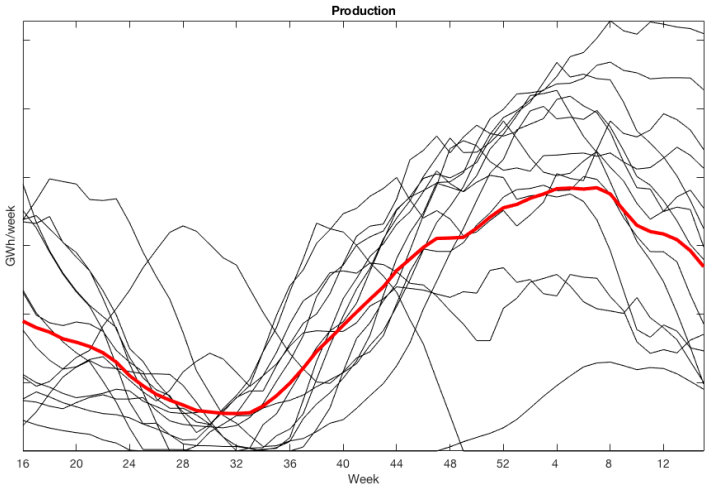

Figure 4.3: The production for the years 2002-2012 are plotted as black curves, while the mean is plotted in red. The plot shows weekly measurements. The data is smoothened to accentuate the trends.

is clearly variations for the different years. One year there is a peak at week 28. In this year the inflow is very big and there is a big production to avoid overflowing the reservoir. In this case the production is high even though the price is low, but it is still more valuable to produce the electricity at a low price than let the reservoir overflow. Despite yearly variations, the average in red shows that there are clear seasonal trends.

4.4 Snow reservoir

Measuring the snow in an area is not easy because it depends on weather, wind, terrain and temperature. There are many different ways to measure the snow. One way is to take measurements in some places in the snow reservoir and use an algorithm to estimate the total amount of snow in the catchment area Lundberg et al. (2008); Marshall and Koh (2007). Then the point measurements can be taken with radars which finds the snow water equivalent(SWE) in the area. The SWE is a measurement of snow, that uses both the density and the thickness to give an exact measurement of the amount of snow. As an example, Nea and Nidelva power plant in Sør-Trøndelag uses this method. Figure 4.4a shows an overview of the catchment area and the

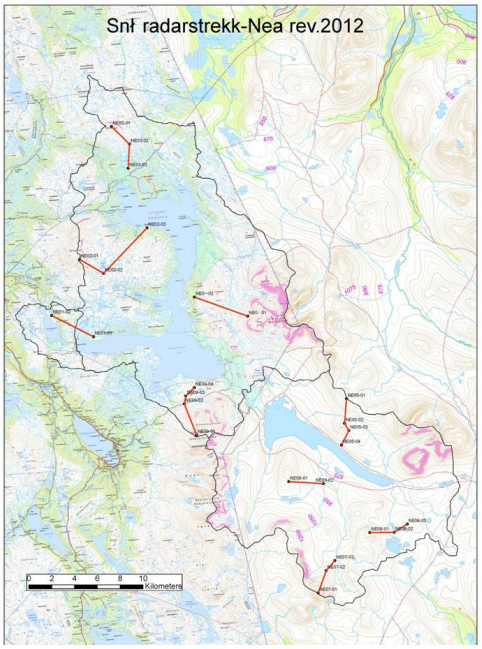

(a) The map of the catchment area in Nea in Sør-Trøndelag.

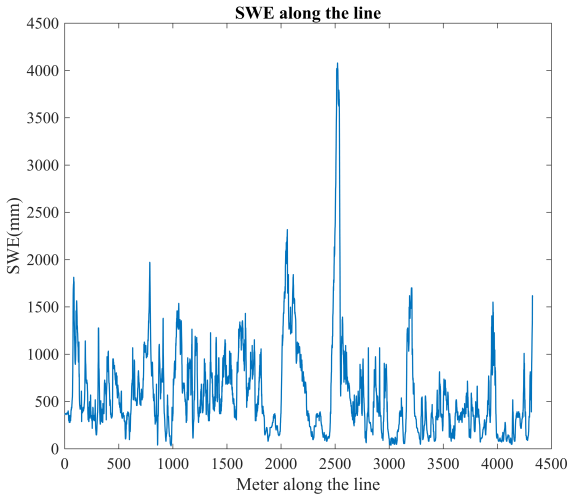

(b) The radar measurement of the SWE along one of the lines at the map.

Figure 4.4: The catchment area for Nea area in Sør-Trøndelag is inside the grey lines. The red line represent the area where the snow is measured by a radar.

red lines where the snow is measured. From the SWE along the lines, the total snow in the area is estimated. Figure 4.4b shows the SWE along one of the lines.

Other models are based on weather forecasts and satellite pictures to estimate the snow reservoir Kolberg and Gottschalk (2010, 2006). The method used to measure the snow reservoir at the relevant power plant is simple, but robust. It is calculated by watching the inflow and the rainfall in the catchment area and calculates the difference between the two. It is based on the assumption that all the rainfall will either be stored as snow in the catchment area or inflow to the reservoir. The error estimate is assumed to be around 10-20 %.[3]

The snow reservoir for the discussed power plant is showed in Figure 4.5. The y-axis is the energy equivalent to the snow in the catchment area, while the x-axis describes which week of the year it is. The black lines are the snow the different years, while the red line represents the average.

[3]Based on communication with an expert from the relevant power plant.

The horizontal line represents no snow. The values under this line is measured to be negative, and are caused by uncertainty in the measuring. The snow reservoir is at the maximum or close to the maximum in the spring, around week 16.

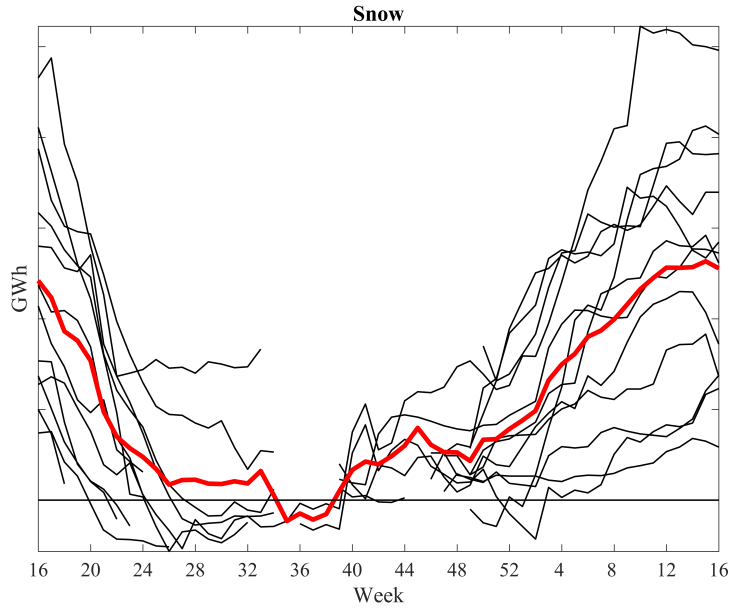

Figure 4.5: The snow reservoir for 2002-2012 are plotted as black curves, while the mean is plotted in red. The plot shows weekly measurements.

By comparing the maximum amount of snow with the total inflow, one assumes that 7-35 % of the inflow is from melted snow. This is only the case if all the melted snow ends up in the reservoir. By taking evaporation and groundwater into account, the actual number will be a bit lower.

4.5 Inflow

Measuring or estimating the inflow is difficult and one of the most uncertain measurements for a hydropower plant. This is because the inflow can come from many different sources. For most reservoir there is a big river that transports the biggest part of the inflow, but there are also multiple small rivers, rain water and water from the ground. All these sources will together make the total inflow. This makes it hard to measure the total inflow to the power plant.

The power plant discussed in this case calculates the inflow by measuring the reservoir level at the start and end of the week and the production. Then the following equation is used: Inflow = Reservoir at the end of the week - Reservoir at the start of the week + Production. Since the measuring mistakes are caused by wind and snow, it is a bigger probability for measuring mistakes through the winter season. In spite of these uncertainties, the error is estimated to be less than 5%[4]. Since the inflow is calculated from the reservoir levels and the production, there is no control of the water balance. This makes it difficult to check if the measurements are correct. An error in the one of the three measurements result in an incorrect amount of inflow. This will also influence the estimation of the snow reservoir since the inflow is used to estimate it.

The inflow for the Norwegian power plant is plotted in Figure 4.6. The black curves represent the yearly inflow, while the red curve is the average. The horizontal line represents no inflow. The measurements that lies under this line is most probably caused by measuring mistakes. The figure shows the inflow has yearly variations due to seasonal variations. The inflow is biggest at the spring because of the snow melting and much lower in the summer. There is also more inflow in the autumn because of the the rain. In the winter it is very little inflow because of the cold temperatures. This seasonal variations will be different for every power plant because of different climate, location and geological profile. In other countries these will have a completely different structure because of different climate.

Fitting the model of the inflow

In the method described in Chapter 3, the K inflow-scenarios are estimated. To do this, a normal distribution is used. The mean, μ, standard deviation, σ, and the correlation coefficient ρ are estimated from the data. The estimation of the mean and the standard deviation is found by

[4] Based on communication with an expert from the relevant power plant.

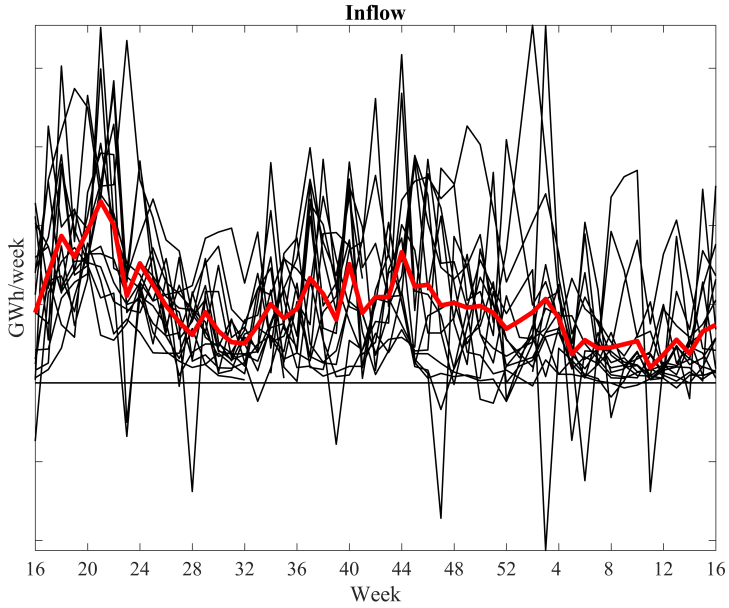

Figure 4.6: The weekly inflow for 2002-2012 are plotted as black curves, while the mean is plotted in red.

using the standard formulas for sample mean and variance, (Walpole et al., 2012, p. 11)

$$\hat{\mu}_t = \frac{1}{N}\sum_{n=1}^{N} q_t^n$$
$$\hat{\sigma}_t^2 = \frac{1}{N-1}\sum_{n=1}^{N} (q_t^n - \hat{\mu}_t)^2.$$

The N is the number of years and the t represent the different time steps. In this case the values are measured every week so t = 1 to 52. The μ_t is the mean for week t and σ_t is the standard deviation for week t. The more years of historical data that are used in the calculations, the better is the approximation. The covariance matrix is then calculated by the formula:

$$\Sigma(\rho) = \begin{pmatrix} \sigma_1 & & & & \\ & \sigma_2 & & & \\ & & \ddots & & \\ & & & \sigma_{51} & \\ & & & & \sigma_{52} \end{pmatrix} \cdot \begin{pmatrix} 1 & \rho & \rho^2 & \rho^3 & \cdots & \rho^{52} \\ \rho & 1 & \rho & \rho^2 & \cdots & \\ & & \ddots & & & \\ & & & \ddots & & \vdots \\ & & \cdots & \rho & 1 & \rho \\ & & \cdots & \rho^2 & \rho & 1 \end{pmatrix} \cdot \begin{pmatrix} \sigma_1 & & & & \\ & \sigma_2 & & & \\ & & \ddots & & \\ & & & \sigma_{51} & \\ & & & & \sigma_{52} \end{pmatrix}.$$

The ρ is found by maximizing the likelihood function. The likelihood is plotted in Figure 4.7, with the maximum marked as a red circle.

$$l(\rho;q) = -\frac{N}{2}\log|\,\Sigma(\rho)\,| - \frac{1}{2}\sum_{n}(q^n-\hat{\mu})'\cdot\Sigma(\rho)^{-1}\cdot(q^n-\hat{\mu})$$

Now, the inflow can be simulated by using $q \sim \mathcal{N}(\hat{\mu},\hat{\Sigma})$. Because of the normal distribution

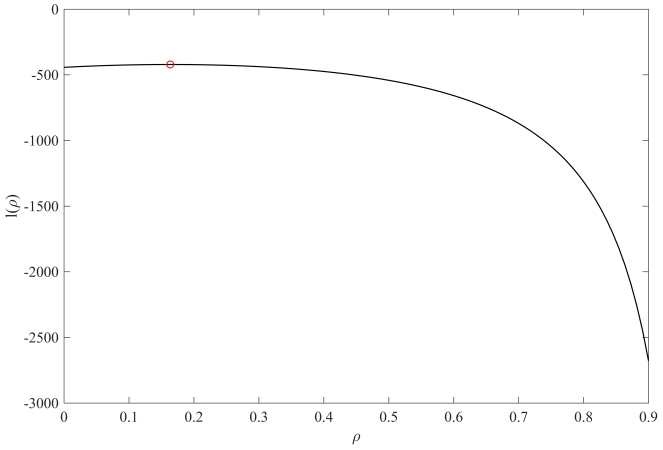

Figure 4.7: The likelihood function is plotted for many different values of the correlation coefficient ρ. The maximum likelihood is denoted with a cross and is obtained with $\rho = 0.19$.

can obtain negative values this have to be treated carefully. There is no physical meaning with a negative inflow in this case. One possible solution is to set all the negative inflows to zero. Since the mean is higher than zero for all the weeks, there will not be a big part of the inflows that are negative. If this had been the case, it would be more appropriate to use another way to estimate the inflow.

The variance is high and the correlation is low. This means that the data variates much each time step. The inflow at the first time step does not give a lot of information about the inflow the next weeks. The inflow is influenced by many factors, which is why the variance is high. Some of these factors are: temperature, rain and amount of sunlight. All of these factors also influence how fast the snow will melt (Otnes and Ræstad, 1978).

Realistic vs fitted data

The simulated data is compared with the realistic one to see how good the estimation fits the real data. Table 4.1 shows some summary statistics for the two cases. This shows that the relative

Table 4.1: The relative error of the original inflow, q and the simulated inflow $\hat{q}$.

$RelErr(\sum_{i=1}^{16} q_i)$	$RelErr(\sigma(\sum_{i=1}^{16} q_i))$	$RelErr(\sum_{i=1}^{52} q_i)$
3.7	22.7	1.1

error for the mean is 3.7 % which is low. This is probably caused by the correction of the negative values in the fitted inflow. For the standard deviation, the relative error is 22.7% which is some higher. The variance for the simulated inflows are a bit bigger compared to the original data. The relative error of the total inflow for one year is only 1.1%. A plot to compare the different inflow data is showed in Figure 4.8. It shows the cumulative probability distribution for the sum

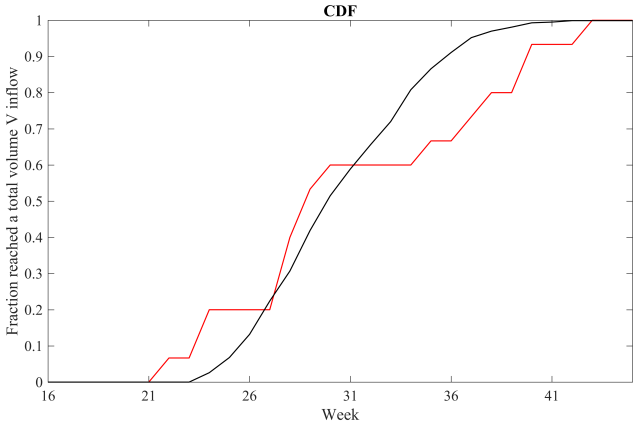

Figure 4.8: The fraction of total inflow that have reached a volume V, plotted for both the real data(red) and fitted inflow data(black).

of the inflow the first weeks: $P(\sum_{t=1}^{w} q_t < V)$, where V is a chosen value. The red line represents the historical data and the black line represents the fitted normal distribution. By the result of Table 4.1 and Figure 4.8 the fitted data are assumed to be a reasonable approximation of the realistic inflow.

4.6 Snow and inflow

In the calculations of the VoI, the inflow-scenarios are divided into groups related to different snow levels. To be able to do this, the snow measurements and the inflow data has to be analyzed. To begin with the data is plotted in the melting period. This is showed in Figure 4.9 and 4.10. Figure 4.9 shows the snow measurements for the melting period. As the figure shows, the snow reservoir is decreasing quite consistently in the melting period. The snow melting from the catchment area will contribute to an increased inflow. This will together with the rainwater make the inflow at the spring bigger than for the rest of the year. After ten weeks, most of the snow reservoirs are close to zero, which means that most of the melting water is either in the reservoir or moving towards the reservoir. Figure 4.10 shows that the inflow starts to increase

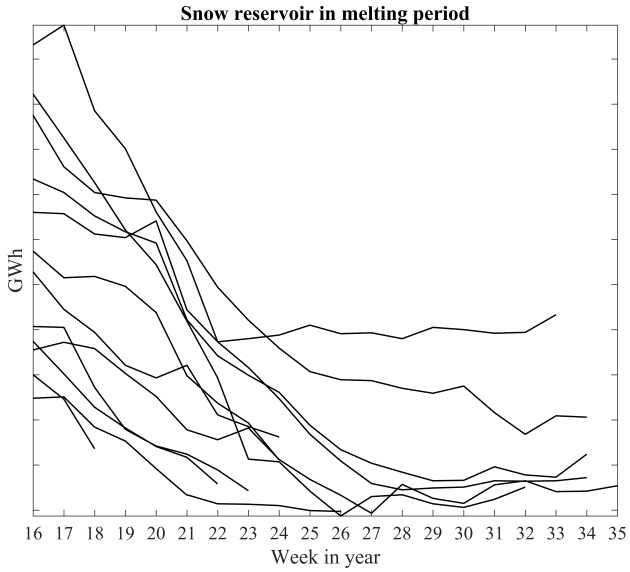

Figure 4.9: The snow reservoir for the first 20 weeks for the years 2002-2012 is plotted.

at the start of the plot, the reaches a maximum around week 20 and then decreases again. This represent the melting water from the snow reservoir that makes the inflow peak in the spring. By looking at the Figure 4.9 it is also possible to see that there is around week 20-22 that the curves are decreasing most rapidly. This means that this is the time were the snow is melting fastest and fits good with the peak of the inflow at the same time. As viewed in the figure, the form and amount of the inflows are different each year. The red curve is an example of a year with small snow reservoir. The inflow is not increasing as much and the melting period starts quite late.

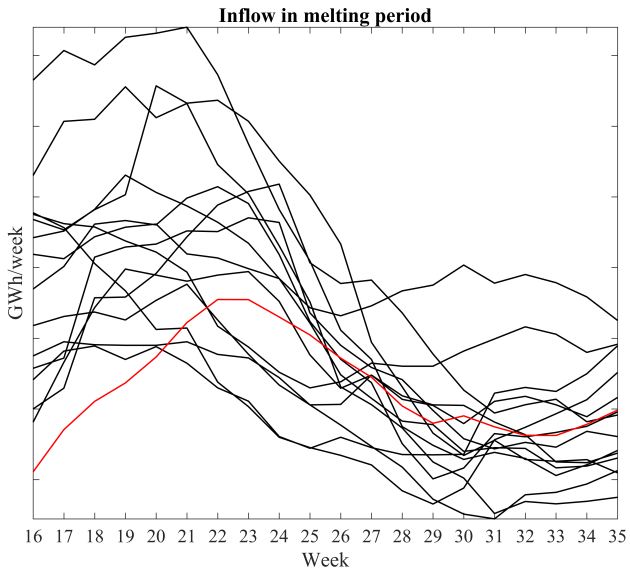

Figure 4.10: The inflow in the melting period.

Like this example shows, the inflow is influenced of the snow reservoir, but also on the weather. The temperature in the spring influences the form of the inflow curve.

Snow and inflow correlation

By analyzing this data it is possible to find out how the inflow and the snow reservoir are correlated. This is an important part of the method since the inflows later are divided into groups based on this relation. To start with, a regression is done to see if the snow measurements and the inflow are correlated. The maximum value for the snow reservoir the first 16 weeks are used as one variable. For the inflow the sum for the j first weeks are used, $j = 1:52$. The j different correlation coefficients are calculated and plotted in Figure 4.11. This shows that the snow and the inflow is most correlated in the first 16 weeks. The red line represent no correlation. If the inflow in Figure 4.10 is studied, the melting period is also finished after around 16 weeks, and the dry period in the summer begins. This is used in Chapter 5 in the numerical testing of the method. A correlation at 0.85 shows that there are a clear trend between the snow measurements and the inflow the following 16 weeks.

The snow will always contribute to a flood of water in the spring, but the fraction of the total

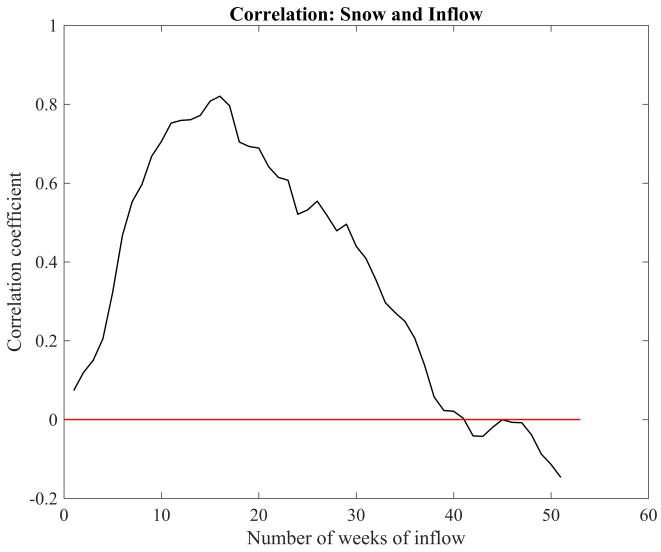

Figure 4.11: The correlation coefficient between the snow measurements and the sum of the j first values of the inflows is plotted. j varies from 1 to 52.

inflow that is originating from the melted water will vary much between the different power plants. In this case, the maximum measurement of the snow reservoir is in average 15% of the total inflow for one year. This means that the snow reservoir is not as big compared to the total inflow. For the 16 first weeks, the melted snow is 49% of the total inflow. This is consistent with the earlier result about the correlation between the snow and the inflow.

Chapter 5

Numerical Results

The method described in Chapter 3 was implemented in MATLAB (MATLAB, 2016). The main numerical results from the numerical testing are presented in this chapter.

5.1 Scheduling

The main goal of Algorithm 1 is to make a decision whether it is valuable to produce a bigger or smaller amount of electricity with the spot price at the time. Figure 5.1 shows two examples of how the price and the average lowering decision vary together. The figure shows this relation for the mean price from the years 2002-2012 at the left side and the price from 2004-2005 at the right side. If the method works perfectly there will always be produced much energy when the spot price is high, and little energy when the spot price is low. The plot shows the price on the right y-axis and the decision on the left y-axis. If the decision at time t is near the top of the y-axis, it means that almost 100 % of the scenarios produce the biggest amount of energy possible. If the decision is near the bottom of the y-axis, then almost every scenario produces the smallest amount of electricity. The decisions are made as a compromise of avoiding the limit and the penalty that follows and the best exploitation of the spot price. By looking at the figure the tendencies are as expected. Both of the plots show that the decision and the price are strongly correlated. Even though the price and the decision are varying together, the decision does not go very close to the upper and lower part of the y-axis. This means that the power plant will in average not very often produce maximum and minimum amounts of electricity. In the plot at

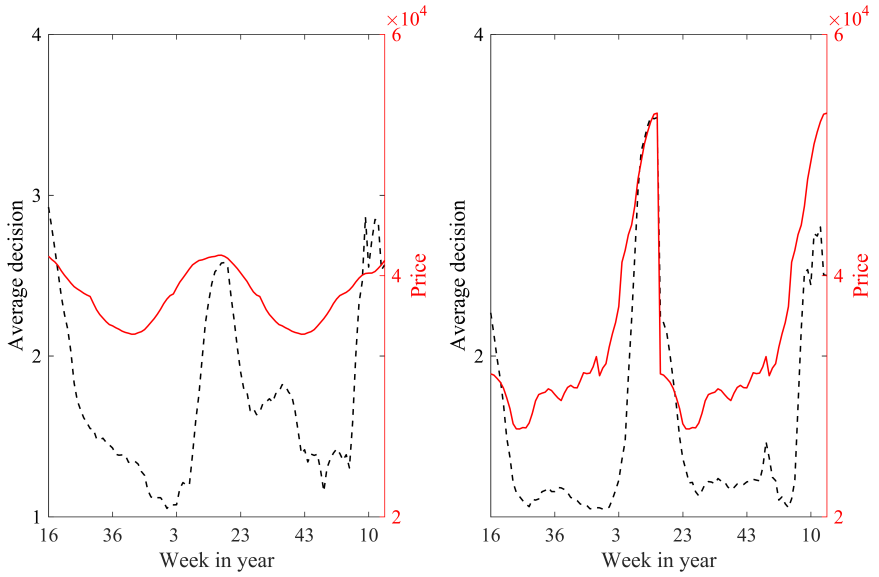

Figure 5.1: The spot price and decision rate are plotted. The x-axis shows the time steps, as weeks in the year. The y-label shows at the left side shows the average decision for the K scenarios and the right side shows how the price varies. The left plot uses the mean spot price from 2002-2012 while the right plot uses the spot price from 2004-2005.

the right side, the price vary a lot more than at the left side. By looking at the decision curve it is possible to see that the curve is closer to the extrema when the price varies more. The choice of the lowering volume is now more based on the spot price, rather than avoiding the penalty zone. This is because there are more money to loose by making the wrong decision.

For the two prices, the forward optimal strategy is plotted in Figure 5.2. As expected from Figure 5.1, the variations are more extreme for the case where the spot price varies more. This results in reservoir levels going closer to the lower and upper limits when the price varies more. In both cases the reservoir levels are not so close to the reservoir limits. This is because of the penalized payoff function, which make the solution avoid the limits. When the price variates more, the price gets more important compared with avoiding the upper and lower limits. An extreme case is tested to see how the method reacts on a price that varies very much. This is done to see whether the reservoir limits gets closer to the limits or not. When the price is varying as a sinus curve between 0 and 200, the reservoir level does not reach the upper or lower limit. Even though a bigger average inflow is used, the result becomes the same. By comparing with the historical reservoir levels, the reservoir levels should be going closer to the limits.

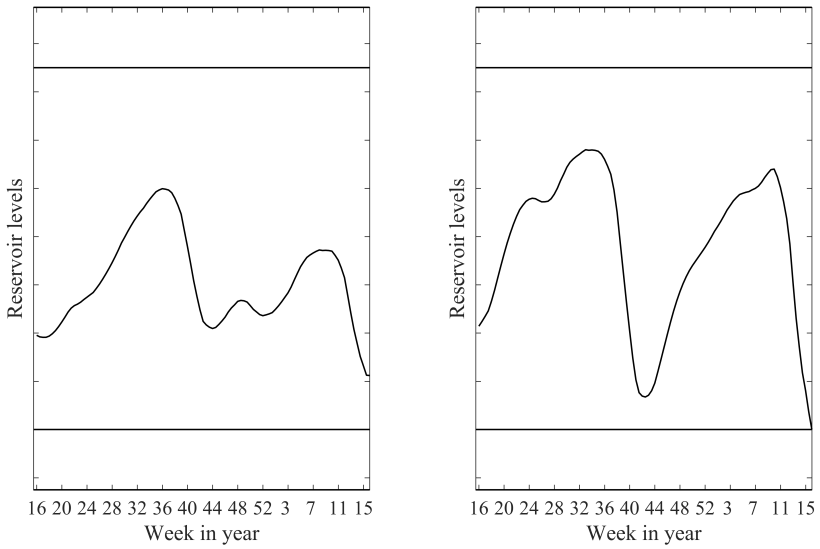

Figure 5.2: The forward optimal strategy is plotted for two different price scenarios. The one at the left uses the mean price for the years 2002-2012, while the one at the right uses the price from 2004-2005. They both have the same initial volume, L_0.

Burn-in period

Since the method is based much on the spot price at the time and how it is compared to the previous spot prices the method does not work well near the time horizon. Here, the method has few spot prices to compare with, so the decisions are mainly based on staying away from the reservoir limits. After some time steps, the method has more spot prices to compare with and can decide whether the current spot price is good or not. This period at the start is called a burn-in period and is showed in Figure 5.3. The last ten weeks of the plot shows a non-smooth and rapidly varying decision rate plotted in black. This happens even though the price, in red, does not change a lot. Numerical testing shows that the burn-in period usually lasts between 5 and 20 weeks. If the goal is to evaluate a period of one year the time horizon should be chosen to be two or three years to avoid the influence of the burn-in period.

Different lowering possibilities

The method is implemented with two and four different lowering possibilities. By using four lowering possibilities, the method becomes more flexible. Because the adjustment is better with four alternatives, the strategy is more optimal. This also makes it possible to include a bigger

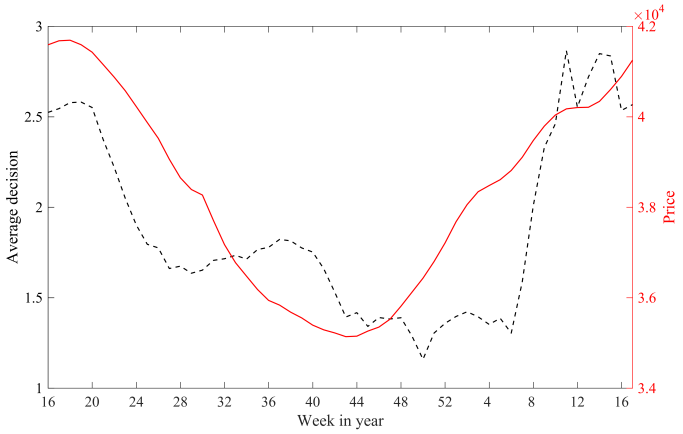

Figure 5.3: The first year for the solution is plotted to illustrate the burn-in period at the start of the algorithm. Since the algorithm is going backwards, this is at the right side of the figure.

range of lowering possibilities. For the case with only two lowering possibilities, the method is depending more on the choice of the two levels. This is illustrated in Figure 5.4. a_1, a_2 and a_3

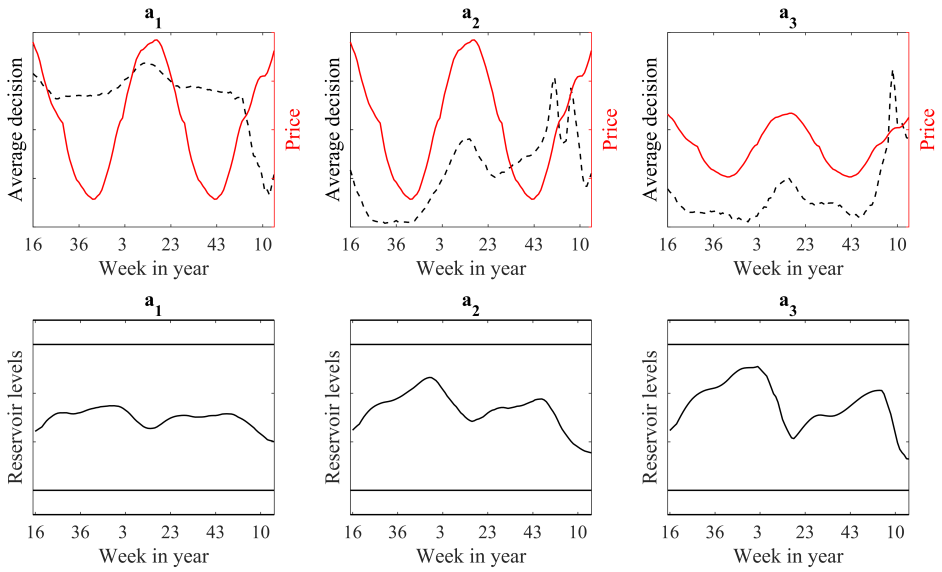

Figure 5.4: For tree different values of the biggest lowering value, the optimal strategy and the decision rate are plotted.

are the different pairs of production levels. The lowest production possibility is constant, while the biggest is increasing for each of the three cases, a_1, a_2 and a_3. By comparing the plots with the different production levels, it is clear that the result varies for the three cases. This is also showed if the relative VoI is calculated, showed in Table 5.1. This shows that even though the

Table 5.1: The relative VoI is calculated for three different lowering situations. There are two lowering possibilities in the example, the lowest is constant, while the biggest is increasing for each of the three cases.

	a_1	a_2	a_3
VoI	0.43	0.68	1.0

optimal strategies have the same trend, there are a big difference in the calculated VoI. More lowering possibilities makes the method more stable and less dependent on the choice of the lowering possibilities.

Stability

The method was tested for many years to see whether it is stable or not when the time horizon, T, is big. The same spot price is used for all of the years, to easier be able to compare the different years with each other. Figure 5.5 shows the method used for ten years. The optimal strategy is almost identical every year, except for the burn-in period. This means that there are no or very little drifting when the method is used for many years.

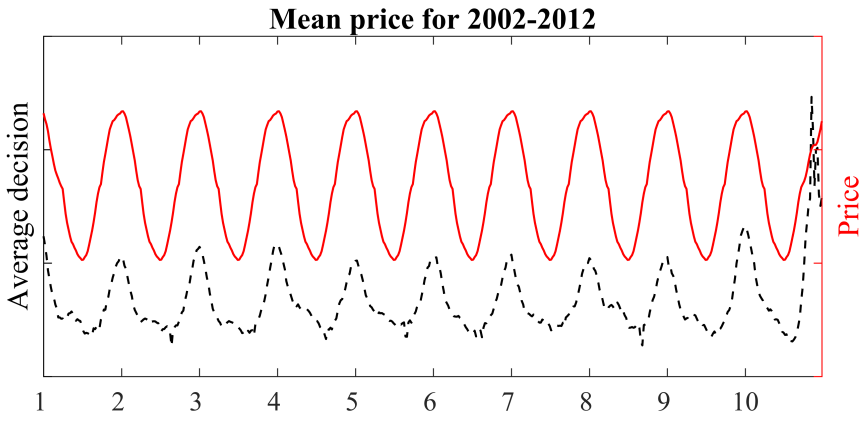

Figure 5.5: The decision and price for ten years.

5.2 VoI

In this section, the VoI is calculated and studied for many different situations. This is done by using the method described in Section 3.2 and variating the different parameters in the model. The

method was implemented with two and four production levels. All the numerical testing were done with $K = 50000$ to minimize the Monte Carlo variations discussed earlier in this chapter. The calculated values of the VoI presented in this chapter are the mean of ten different simulated inflows. The numerical results presented are assumed to be stable and reliable. Numerical testing showed that the value of the total production one year increased between 0 and 10 % by including the snow measurement. In this section, different parameters and variations are studied to see how they influence the VoI.

Initially, the different number of lowering possibilities was studied. The relative VoI is presented in Table 5.2 and in Figure 5.6. The result shows that the VoI always was bigger when four lower-

Table 5.2: The VoI is calculated for two and four lowering possibilities and the relative numbers are presented.

Classes	3	6	9	12
2 lowering possibilities	0	0	0.09	0.21
4 lowering possibilities	0	0.23	0.47	1.00

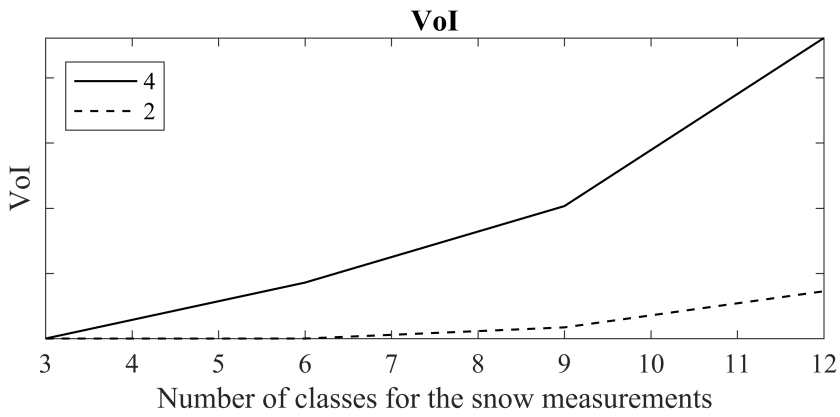

Figure 5.6: The mean value of the VoI is plotted for different classes for the method used with two and four lowering possibilities.

ing possibilities were used. As earlier mentioned, this difference is caused by a bigger flexibility and better adjustment of the strategy. Because of this result, the method with four lowering possibilities are used further in the numerical analysis.

Different number of classes

The number of classes, Y, used is 3, 6, 9 and 12. By using the same inflow scenarios q in all the different number of classes it is easier to see how this affects the VoI. The result is showed in Figure 5.6. For $Y = 3$ the VoI becomes zero for both two and four lowering possibilities. For each of the classes an optimal strategy is found. By looking at these different strategies, they are all very similar and none of them are near the upper or lower limits. This means that even though the inflow is big or small, the reservoir is big enough to store all the inflow. By looking at the historical data and the number of overflow, it can be verified that the reservoir is quite big compared to the inflow. When the price is low, the production is also low, they are not forced to sell at a low price to avoid overflow. Because of this, the decisions are then based mostly on the price, which result in similar strategy for different snow measurements. When the VoI is calculated there is one strategy that gives the maximal payoff for all of the different levels of snow. This make PV = PoV, and the VoI becomes zero. By letting the number of classes increase, each inflow scenario becomes more separated and there is a bigger chance that the VoI is bigger than zero

The number of classes should be decided by evaluating how precise the snow measurements are. In the previous part, the snow measurements are assumed to be correct and with no error. The analysis in Chapter 4 showed that zero error is not realistic. How measuring errors can influence the result is showed by studying an example with three and nine number of classes. Figure 5.7 shows the mean of the inflow for each class. Three classes are used in the left plot and nine classes are used in the right plot. The different classes lie much closer to each other when there are nine classes. This makes the method vulnerable for measuring mistakes. If there are measured 30% more snow than in reality, the inflow is simulated to be around 30 % bigger than it is in reality and probably placed in the wrong class. This error is more likely to happen when the mean value for each class lies close to each other. Then it will be safer to choose three or six classes. If the snow measurements are more precise, the simulation of the inflow is simulated to be approximately the same as the realistic one. In that case, a more detailed division of the inflows will be more realistic.

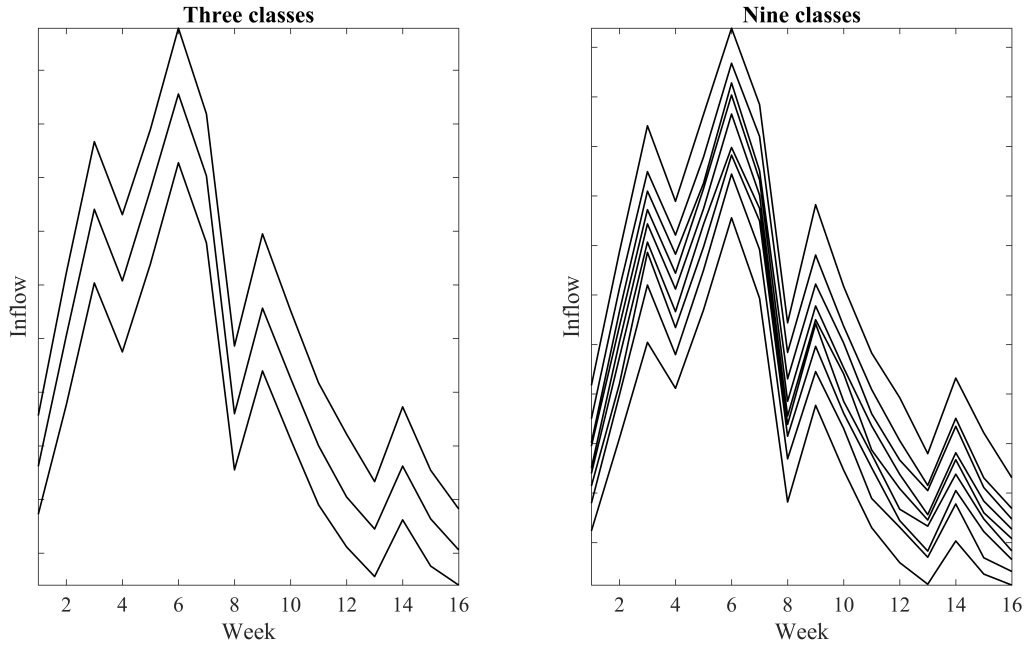

Figure 5.7: The mean inflows for three classes are plotted at the left side, while the mean inflows for nine classes are plotted at the right side. The two cases uses the same K scenarios before the division into classes.

Monte Carlo variations

Because of the simulated inflow, there will be some variations in the optimal strategy and the VoI. By looking at the parameters in the normal distributions, the variance are quite big and the correlation small. This result in bigger variations in the simulated inflow. The variance in the VoI should be getting smaller if the sample size K increases. To see how the variations depend on the number of scenarios, the algorithm is tested with both 5000 and 50 000 scenarios. This was done ten times and the VoI was analyzed. The change of the standard deviation and the coefficient of variance for both of the cases are shown in Table 5.3. The coefficient of variance is calculated by the formula $c_v = \frac{\sigma}{\mu}$. This shows that the variation decreases with 90.1 % when the

Table 5.3: Change of mean, variance and coefficient of variance for the VoI for 5000 and 50 000 scenarios caused by Monte Carlo variations.

	μ	σ	c_v
Percentage change	-2.3	-90.1	-90.9

number of scenarios increases from 5000 to 50 000. The method gets much more precise when the number of scenarios increases. If the method is used with a low number of scenarios, the Monte Carlo variations can make the results incorrect.

5.3 Sensitivity analysis

It is interesting to study the sensitivity of the VoI. This can be done by varying different parameters in the model and see how the VoI changes. The sensitivity analysis can give more information about when the snow measurements are valuable. In this section the method is used with four lowering possibilities to make the situation more similar to the real situation.

To begin with the upper limit is variated. One assumption is that if the risk of overflow is big, the need of an optimal strategy is more important and the snow can bring more information. To test this hypothesis, the VoI was calculated for many different upper limits $\frac{L_{max}}{L_{max,original}} = [0.50, 0.60, 0.70, 80]$. Table 5.4 shows the VoI for the different upper limits. The table shows that

Table 5.4: The VoI is calculated for different ratios of the upper limits $L_{max}/L_{max,original}$.

$L_{max}/L_{max,original}$	0.50	0.60	0.70	0.80
Relative VoI	1.0	0.82	0	0

the VoI is positive when the upper limit is 50 and 60 % of the original one. This means that the hypothesis is correct and the values of the measurements are bigger if the risk of overflow is high.

Sensitivity of the snow measurements

Another aspect that is very interesting to study at is the uncertainty of the snow measurements. As discussed in Chapter 4, the uncertainties can be big for these measurements. By including different uncertainties, the VoI can be studied for the different cases. This is done by changing some of the inflows under the division of the classes. By doing this the snow reservoir gives less information and the VoI should be lower. If there are three classes $\{low, medium, high\}$ and

the snow is measured to medium, there is normally medium inflows. In this case on the other hand, some of the inflows originating from low and high snow reservoir is included in the inflow for medium snow reservoir. This means that if the measurement shows that there is medium snow, there will still be a probability that the inflow is small or big.

Figure 5.8 shows how some of the inflow have changed class. On the left side, the original division is showed and on the right side, some of the inflows have changed class. In this case only a small bit of the inflows have changed strategy. The VoI is calculated for three cases: the standard way, with 40% of the inflow mixed with the neighbor-class and a non-sorted inflow. For the non-sorted inflow, it is drawn directly from the normal distribution and divided into groups. In this case the snow measurements give no information and the VoI is expected to be zero. For the case with 40% of the inflow mixed, the VoI is expected to be lower compared to the standard case.

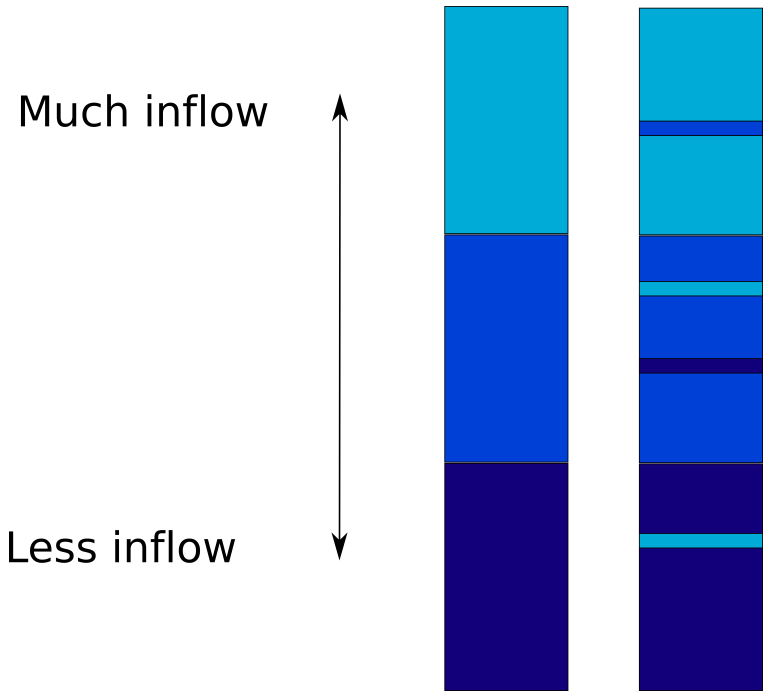

Figure 5.8: The three different classes at the left side is the division where all inflows are measured correctly. At the right side, the uncertainty in the measurement of the inflow cases some errors in the division. Some of the inflows that are expected to be small, are medium, etc.

The result is showed in Figure 5.9. The x-axis represent the number of classes, and the y-axis the

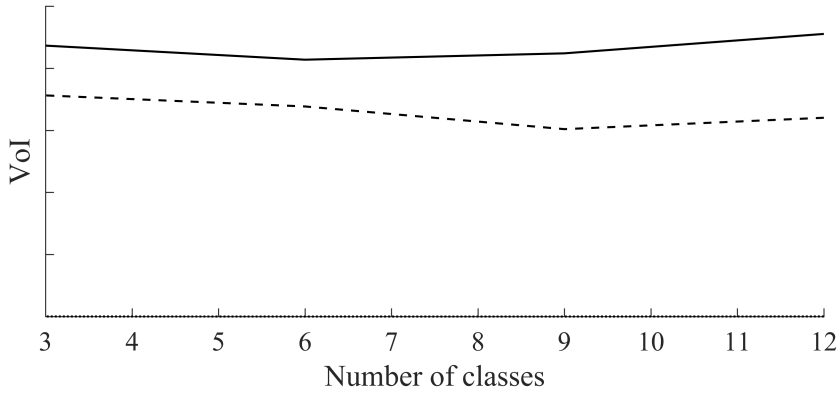

Figure 5.9: The VoI is plotted for two different cases to study the sensitivity. The solid line represent the normal case and the dotted line represent the case were 40 % of the inflow in the different classes have switched to a neighbor class.

VoI. The thick line represent the case where none of the inflows are changed, the dashed line(- -) represent the case where 40 percent of the inflow have changed class and the dotted lines (...) represent the case where 100 percent of the inflow is mixed up. The VoI for the original case is higher than the case where the classes are mixed for all of the different classes. The VoI for the total random inflow became zero. This shows that if all the different snow measurements result in very similar simulated inflows, the measurements does not have any value. The VoI decreases with 25 % for the case where 40% of the inflow is in the wrong class. This difference becomes bigger with an increasing number of classes. This can be caused because a higher number of classes, means a better division of the different inflows. If the division is finer, the inflows are more separated by the snow measurements. This result in a bigger difference in the VoI.

Sensitivity of the correlation between the snow and inflow

A last thing that is tested is the number of weeks that is used in the division of the classes. From Figure 4.11 the number of weeks with highest correlation were found to be 16, but this value can also be changed. Since the correlation is less for all other alternatives, all of the calculated VoI should be lower than the original one. The VoI is calculated by using 4, 16 and 24 weeks in the division of the inflow. The correlation coefficient for the different cases are 0.25, 0.85 and 0.55 respectively. The result is showed in Figure 5.10. The figure shows the three different cases plotted together. The solid line represent the original case, the dashed line represent the case

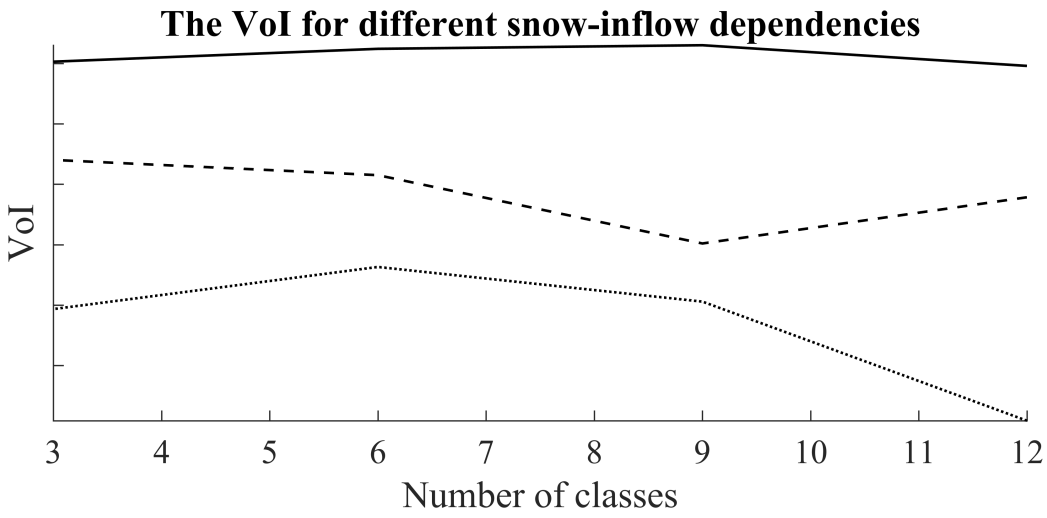

Figure 5.10: The solid line represent the VoI for the original case, the dashed line(- - -) divide the inflow after 5 weeks and the dotted line(...) divide the inflow after 24 weeks.

where 4 weeks of inflow is used in the division and the dotted line is the case with 24. The solid line lies above the other two for every number of classes, as expected. The snow measurements and the inflow are most correlated for 16 weeks. The VoI decreases in average with 24 and 60 % for a correlation coefficient equal 0.25 and 0.55 representatively. The inflow scenarios used to calculate the VoI in Figure 5.9 and 5.10 are not the same, so the solid lines vary a bit because of variations in the simulations.

5.4 VoI versus cost of taking the measurements

After studying the VoI, the numerical testing showed that if the reservoir level is small compared to the total inflow, the measurements are very valuable. For the Norwegian power plant, the measurements are calculated using already existing data and is therefore obtained for a very low cost. Since this price is lower than the VoI it is worth to make the calculations. Other power plants may measure the snow by using other methods described in Chapter 4, which have a higher cost. This can be done by using a radar and the snow scooter and then using an algorithm to estimate the total snow reservoir. The first time cost is high, because the company have to invest in a radar, but in the long run, the average cost will be smaller than the VoI. If the reservoir is big on the other hand, the VoI is small and there is no reason to include the snow

measurements to find the optimal scheduling.

An example is now made to show when different measuring methods are valuable. If the snow is measured and then processed in two different ways, the VoI will become different for the two cases. Method 1 processes the data for a value P_2 and method 2 processes the data less, for a value $P_2/5$. The earned revenue is described by the following equations:

$$Rev_1 = VoI_1 - P_1 - P_2$$
$$Rev_2 = VoI_2 - P_1 - \frac{P_2}{5}.$$

P_1 is the price of acquiring data and P_2 is the price of processing the data. In this example the P_1 and P_2 varies, while the VoI_1 and VoI_2 are constant. Figure 5.11 can be used to decide which of the two methods that should be used to maximize the earned revenue. The red lines

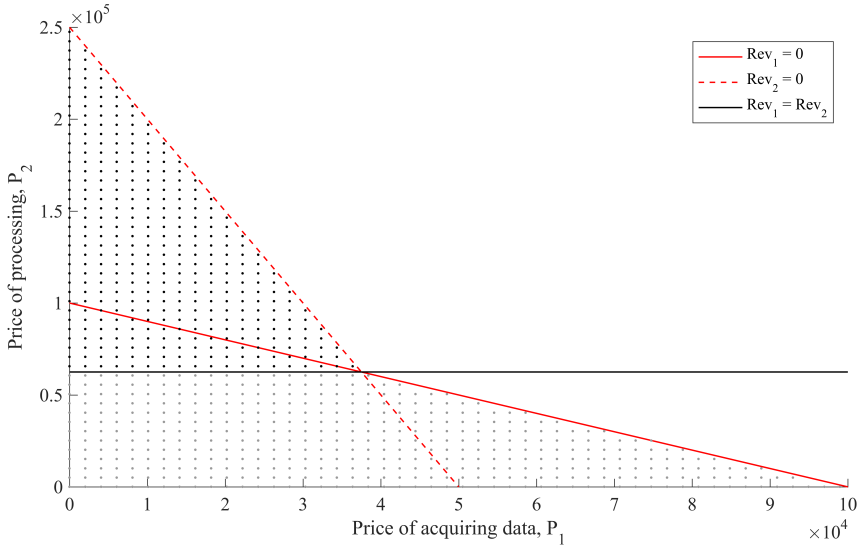

Figure 5.11: Decision regions are plotted for two different methods. In the grey area method 1 gives the highest revenue and in the black area method 2 gives the highest revenue. No measurements are valuable in the white area.

describes the limit where the VoI is equal the price of processing and measuring the data. The revenue is zero over the lines and positive under the line. The dashed line describes the case with $VoI_2 = 5 \cdot 10^4$ while the solid line is for the $VoI_1 = 10^5$. The black line represent where the revenue is equal for the two cases. The black and grey areas describe where the different tests

are optimal. In the black area, the method 2 is the one that gives highest revenue. This means that if the cost of processing data is very high, it would be optimal to process the data less. This means that the VoI is smaller, but the total revenue gets bigger compared to method 1. The grey area represent the area where method 1 gives the highest revenue.

5.5 Run-time

By analyzing Algorithm 1 and 2 it is possible to decide the run-time of the algorithm. Algorithm 1 have run-time $O(TK)$, and Algorithm 2 runs this Y times, so the total run-time becomes $O(KTY)$. This means that the time increases linearly with the number of scenarios, K, the number of time steps, T, and the number of classes, Y. The run-time is plotted in Figure 5.12 by variating K, T and Y separately. This shows that the run-time grows linearly as expected. The

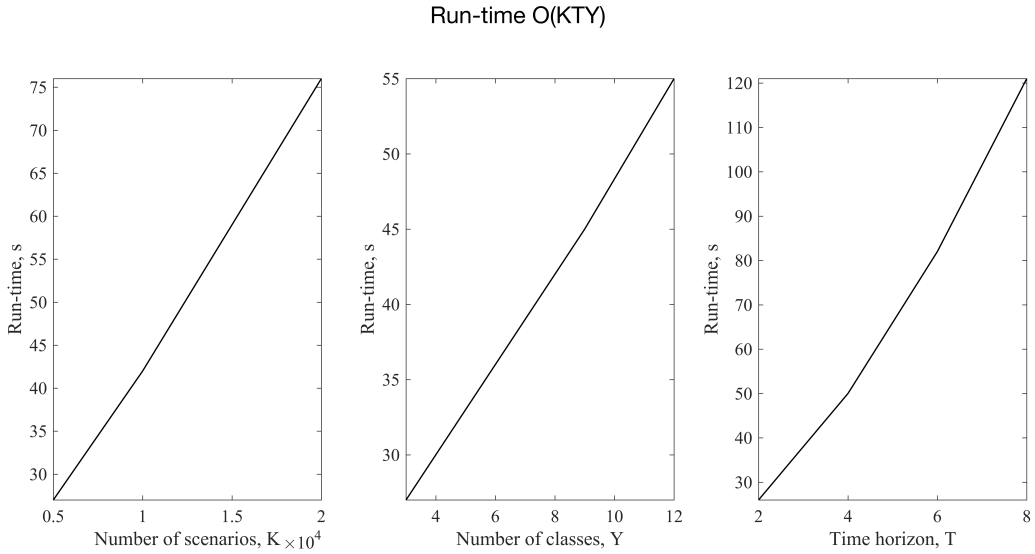

Figure 5.12: The run-time is plotted while one parameter is changed in each of the plots.

running time of the algorithm with $T = 104$, $K = 10000$ and $Y = 9$ is 1 minute and 50 seconds. The numerical testing is done on a Macbook pro, so by using a computer with higher processor speed, the calculations could have been done much faster.

Chapter 6

Conclusion and Further Work

6.1 Conclusion

An approximative LSMC-method is implemented to find the optimal strategy for a hydropower plant. The method uses dynamic programming, simulation and regression in the optimization. The decision of the production at each time step is mainly based on the spot price and the reservoir limits. Numerical testing shows that the penalty for overflow is rather strict, so the optimal strategy never goes entirely to the upper and lower limits. The optimal strategy is then used in the calculation of the VoI. This is done by dividing the snow measurements into classes and then divide the inflow into the different classes. To find out how this division should be done, the data is analyzed. The maximum of the snow reservoir and the sum of the inflow the first 16 weeks of the flood period are strongly correlated with an correlation coefficient equal 0.85. This is later used to divide the inflow into classes based on the snow measurements. By studying the measuring methods for the inflow, reservoir levels, production and snow reservoir, the uncertainty is assumed biggest for the snow measurement. The uncertainty is found to be 10-20 %. The uncertainty for the inflow, reservoir level and production is around 5%.

The numerical results presented in Chapter 5 shows that if the reservoir is big and the probability for overflow is low, the snow measurements are not very valuable. If the reservoir is smaller, on the other hand, and the probability for overflow is higher and the snow measurements are valuable. If the reservoir decreases with 10%, the VoI decreases with 18%(Figure 5.6). With a

smaller reservoir, the strategy gets more optimized for each snow measurement. The numerical testing also shows that the analysis of the data is important in the calculation of the VoI. It is crucial to find how the snow and the inflow are correlated and use this to simulate the inflow. This is also central in the division of the different classes of snow measurements. Testing shows that the VoI decreases with 24 and 60 % when the correlation coefficient decreases from 0.85 to 0.55 and 0.25 respectively(Figure 5.10). By studying the stability of the VoI, the method proves to be quite stable. Even though 40 % of the inflow were put in the wrong class caused by uncertainty in the snow measurements, the VoI is calculated to be positive and around 25% lower than the original case(Figure 5.9). This means that even though the snow measurements in the data analysis have 40 % uncertainty, the measurements are still valuable and can be used in the optimization procedure, if the VoI exceeds the price of data acquisition and processing.

The increase of value caused by the snow measurements are between 0 and 10 %, depending on the parameters in the model. Even though the power plant includes the snow measurements in the optimization process, the measurements can still be better exploited by studying the dependencies between the snow and the inflow. In conclusion, one assumes that the studying of the VoI can increase the revenue for many Norwegian hydropower plants.

6.2 Possible improvements and changes

There are multiple aspects and details that could have been looked more into. First of all, there would have been very interesting to try using another dynamic programming approximative method. By using another method, the optimal strategy could be different and maybe go closer to the upper and lower limits. It would have been interesting to see how this would influence the VoI. Another thing that could have been done differently is the calculation of the VoI. This can be done in many ways, and a different approach should give similar values as the values in the result. If this had been done in two different ways, the values could be compared.

The data used in the thesis consisted of weekly measurements from one power plant from 2002 to 2012. The data analysis could have contained a lot more data, to have a better foundation to

study the dependencies and the trends in the data. This could for example be done for multiple power plants or with data from a bigger time period. The model for the simulation of inflow could also have been done differently. This could for example be done by using an ARIMA-model for the inflow. One critical element is the accuracy of the snow measurements. Given more data, one could imagine fitting a useful likelihood model more formally than what was done here.

It would also have been interesting to calculate an optimization with deterministic inflow. This could be used to see how the optimal strategy is and could be used to calculate $PoV_{perfect}$. This value could be compared with the PoV to see how good the optimization method is.

Appendix A

Acronyms

ARIMA Autoregressive Integrated Moving Average

CDF Cumulative Distribution Function

G Giga, 10^9

IEA International Energy Agency

LSMC Least-Square Monte Carlo

M Mega, 10^6

PoV Posterior Value

PV Prior Value

SWE Snow Water Equivalent

T Terra, 10^{12}

VoI Value of Information

Wh Watt hour

Bibliography

Den Norske Regjeringen (2014). Norsk krafthistorie på 5 minutter. [Online; accessed 21-May-2016].

Denault, M., Simonato, J.-G., and Stentoft, L. (2013). A Simulation-and-Regression Approach for Stochastic Dynamic Programs with Endogenous State Variables. *Computer and Operations research*, 40:2760–2769.

Eidsvik, J., Mukerji, T., and Bhattacharjya, D. (2015). *Value of Information in the Earth Sciences*. Cambridge University Press, 1st edition.

Fosso, O., Mo, B., and Wangensteen, I. (1999). Generating Scheduling in a Deregulated System. The Norwegian case. . *IEEE Transactions on Power Systems*, 14(1):75–81.

Kolberg, S. and Gottschalk, L. (2006). Updating of Snow Depletion Curve with Remote Sensing Data. *Hydrological Processes*, 20:2362–2380.

Kolberg, S. and Gottschalk, L. (2010). Interannual Stability of Grid Cell Snow Depletion Curves as Estimated from MODIS Images. *AGU Publication*, 46:W11555.

Lundberg, A., Granlund, N., and Gustafsson, D. (2008). Towards Automated 'Ground truth' Snow Measurements - A Review of Operational and New Measurement Methods for Sweden, Norway, and Finland. *Journal of Hydrology*, (24):135–142.

Marshall, H.-P. and Koh, G. (2007). Frequency Modulated Continuous Wave(FMCW) radars for snow research. *Cold Regions Science and Technology*, (52):118–131.

MATLAB (2016). *version 7.10.0 (R2016a)*. The MathWorks Inc., Natick, Massachusetts.

Nilsson, A. (2014). Nordic Market Report 2014. [Online; accessed 24-May-2016].

NVE (2016). Grunnvann i Norge. [Online; accessed 24-May-2016].

Otnes, J. and Ræstad, E. (1978). *Hydrologi i praksis*. Ingeniørforlaget, 1st edition.

Powell, W. (2011). *Approximate Dynamic Programming*. Wiley, 2nd edition.

Raghavendra, S. (2013). Instrumentation and Monitoring of Dam and Reservoir. *NITK Surathkal*.

SSB (2015). Elektrisitet 2014. [Online; accessed 17-June-2016].

Statkraft (2015). Årsrapport 2014, Marked og Produksjon. *Statkraft*.

Sucar, L., Morales, E., and Hoey, J. (2012). *Decision Theory Models for Applications in Artificial Intelligence*. IGI Global, 1st edition.

Susskind, H. and Raseman, C. (1970). *Combines Hydroelectric Pumped Storage and Nuclear Power Generation*. Brookhaven National Labaratory, 1st edition.

Séguin, S., Fleten, S.-E., Côté, P., Pichler, A., and Audet, C. (2015). Stochastic Short-term Hydropower Planning with Inflow Scenario Trees.

Wallace, S. and Fleten, S. (2003). Stochastic Programming Models in Energy. *Computer and Operations research*, 10:637 – 677.

Walpole, Myers, Myers, and Ye (2012). *Probability and Statistics for Engineers*. Pearson / Prentice Hall, 9th edition.